CHALMERS

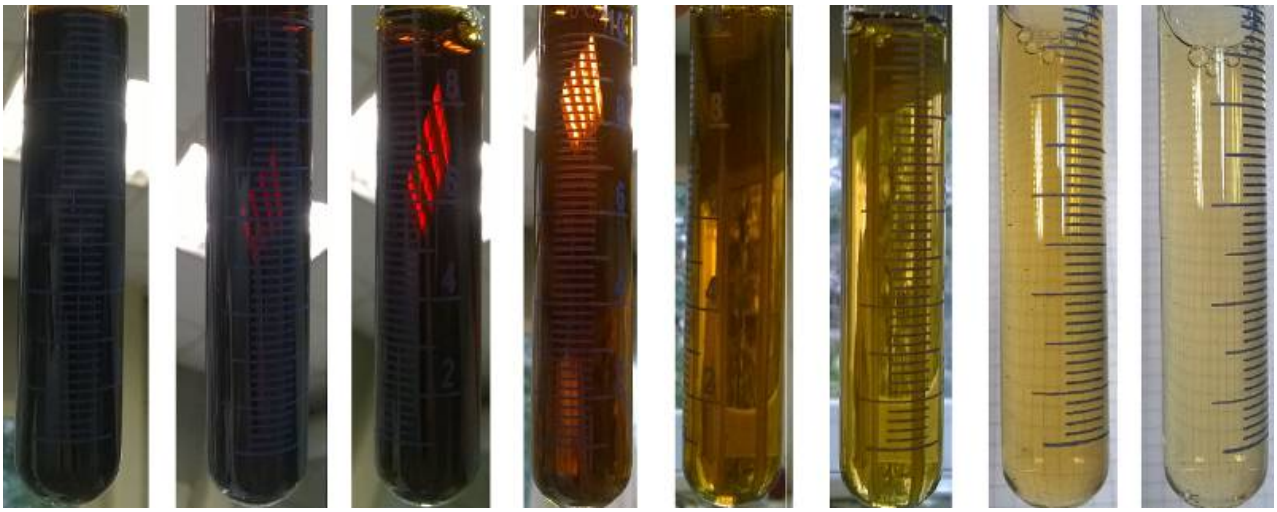

Preparation of polymer coated Magnetite Nanoparticles via Fenton's reagent

Master's thesis in Chemistry and Chemical Engineering

Karsten Mesecke

Department of Chemistry and Chemical Engineering

CHALMERS UNIVERSITY OF TECHNOLOGY

Gothenburg, Sweden 2015

Abstract

Magnetite nanoparticles (MNP) have been intensively studied in recent years with many promising applications e.g. as contrast agent for MRI and magnetic fluid hyperthermia. However there is still demand for stable bio-compatible MNPs suitable for mentioned biomedical applications. The preparation method developed in this thesis combines MNP formation and direct encapsulation within polyvinyl alcohol (PVAL) by using Fenton's reagent. Hydrogen peroxide addition to an Fe^{2+} solution causes formation of nano-sized Fe^{2+}/Fe^{3+} precipitate and simultaneously formed hydroxyl radicals can crosslink PVAL. Furthermore it was shown that only a fraction of nano-sized precipitate is encapsulated within PVAL and a separation step was necessary prior to magnetite formation by ammonia addition.

Obtained dispersions are stable up to 4 wt% of core-shell particles containing 1 wt% magnetite. The size of the magnetite core can be tuned by temperature and pH in between 2-10 nm and the overall core-shell particles exhibit an hydrodynamic radius around 100 nm, whereas one polymer particle can contain several magnetite cores. ESCA/XPS detected only traces of iron oxide in the surface layer, indicating nearly complete encapsulation by PVAL and magnetization measurements confirm expected superparamagnetism without hysteresis.

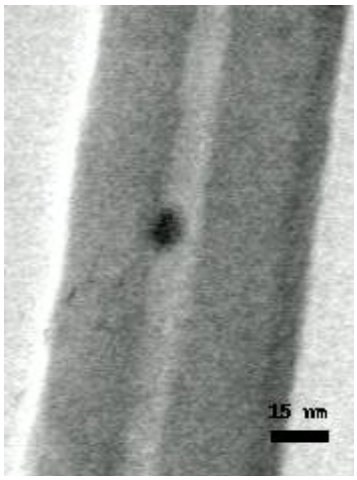

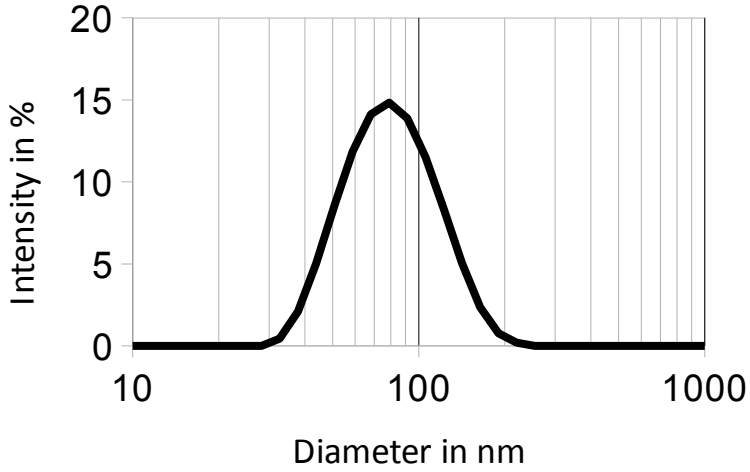

TEM picture of single magnetite core onto carbon grid at 200k magnification, revealing magnetite cores below 10 nm in size (left); DLS intensity distribution of nanoparticles in diluted aqueous dispersion, revealing a hydrodynamic radius of polymer encapsulated magnetite nanoparticles in between 60 nm and 100 nm (right)

Table of Content

1 Introduction

The superparamagnetic behavior of magnetic nanoparticles leads to a variety of applications like magnetic fluids, catalysis, data storage, MRI and magnetic fluid hyperthermia [1,2]. There are different types of magnetic nanoparticles, whereas this work focused on magnetite (Fe_3O_4) nanoparticles (MNPs) for bio-medical applications, especially magnetic resonance imaging (MRI) and magnetic fluid hyperthermia. Magnetite is bio-compatible on its own, but MNPs injected into the bloodstream are rapidly captured by the immune system [3]. In order to reach their desired location within the body they shouldn't exceed a size of 20 nm and they have to be stabilized against protein interaction, preferable by encapsulation with a polymer providing steric stabilization [1,4].

One problem for obtaining an homogeneous polymer shell around the MNPs is their magnetic dipole-dipole attraction [1]. Without any precautions for keeping the nanoparticles apart from each other simple polymerization leads to agglomeration [1]. One possibility would be carrying out the polymerization in a water-in-oil microemulsion [1]. However these particles exceed size requirements for biomedical applications and contain less than 5 wt% magnetite [5]. A totally different approach was developed in this thesis, first Fe^{2+} and Fe^{3+} ions are embedded within crosslinked polyvinyl alcohol (PVAL) by Fenton's reaction and then magnetite is formed by increasing the pH. The problem of agglomeration before encapsulation is circumvented and the bio-compatibility of PVAL is advantageous for bio-medical applications [2].

2 Theory

2.1 Polymers and surfactants in solution

2.1.1 Water-soluble polymers

Water-soluble polymers can be non-ionic like polyethylene oxide (PEO), Polyvinylpyrrolidone (PVP), polyoxazoline (POZ), polyvinyl alcohol (PVAL) or Dextran as well as ionic like polyacrylic acid (PAA) or polymethacrylic acid (PMA) [6,7]. PEO, PVP and POZ are highly water soluble, bio-compatible and applicable in medicine due to their low toxicity [6,7]. Polymer solutions are easily characterized by viscosimetry, also being a suitable method for molecular weight determination [6]. They are less stable than solutions of low molecular weight compounds, whereas long chains separate more easily than shorter chains of the same polymer [6]. For instance the addition of salt can decrease the solubility of polymers in aqueous solution drastically, causing precipitation or so called salting-out [6].

The characteristic of PEO is temperature dependent solubility. It's highly water soluble at low temperatures, but insoluble at high temperatures (e.g. cloud point of PEO $\overline{M}$=8000 g·mol^{-1} is approx. 130°C). This unusual behavior is caused by a decreased polarity due to a conformational change of the ethylene oxide groups [6].

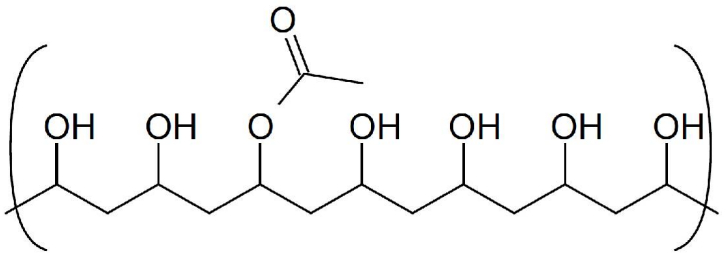

Figure 1 Partially hydrolyzed polyvinyl alcohol with acetate groups

PVAL is as well bio-degradable, bio-compatible and has good functionalization ability which is beneficial for medical applications [2], but its water solubility depends on the degree of hydrolysis [6]. Since it is only produced by hydrolysis of polyvinyl acetate, the degree of hydrolysis is an important characteristic [8]. Partially hydrolyzed polymer with ca. 10% remaining acetate groups as shown in Figure 1, is easily soluble in water, but fully hydrolyzed PVAL is difficult to dissolve [6,8]. Dissolution is favored by heating, because hydrogen bonds have to be broken in the solid polymer, whereas the aqueous polymer solution is also stable at lower temperatures [6]. Moreover it can be crosslinked with boric acid, increasing for example the glass transition temperature [9].

2.1.2 Surfactants

Surfactants are molecules with an hydrophilic and an hydrophobic part, causing assembly at surfaces in order to reduce their overall energy [6]. For example surfactants assemble at the air-liquid interface, lowering the liquids surface tension. There are four groups of surfactants categorized by the polarity of their hydrophilic part: Anionics, Non-ionics, Cationics and Zwitterionics, whereas each is more or less suitable for different applications [6]. Cationics are mainly quaternary ammonium compounds and they strongly adsorb to most surfaces since they are negatively charged [6].

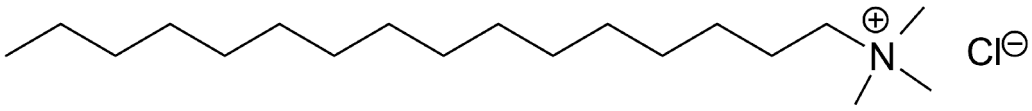

Figure 2 Chemical structure of Cetyltrimethylammonium chloride [6]

Micelles start to form if the surfactant reaches a certain concentration in solution (CMC = critical micelle concentration), the surfactant molecules assemble with each other in order to hide their hydrophobic part from aqueous solution [6]. If polymers are dissolved in the same system, assembly of surfactant molecules is induced at much lower concentration (CAC = critical association concentration) [6], which could also increase the polymers solubility in solution [6].

Moreover there are surface active polymers, which are co-polymers containing several hydrophilic and hydrophobic parts [6]. For example hydrophobic polyacrylates with hydrophilic polyethylene oxide side chains can adsorb onto solid surfaces preventing protein and bio-molecule adsorption [6]. Another well known example are Pluronics which are tri-block co-polymers of polyethylene oxide and polypropylene oxide [6].

2.1.3 Microemulsions

A microemulsion is a thermodynamically stable mixture of two immiscible liquids at high surfactant concentrations [6]. Its formation is promoted by the presence of medium-chain alcohols as co-surfactant or the salt addition. There are oil-in-water, bicontinuous and water-in-oil microemulsions, whereas the latter one is called a reversed microemulsion [6]. The droplet or micelle size is in the nanometer range (e.g. 10 nm), which is beneficial for the formation of nanoparticles [1,6].

Oil-in-water microemulsions are suitable to synthesize polymer nanoparticles whereas the monomer is part of the oil phase [10]. For instance, Wang et al. prepared monodisperse polystyrene particles of 19 nm with sodium dodecyl sulfate (SDS) as surfactant and n-butanol as co-surfactant [10]. Inorganic nanoparticles on the other side require water-in-oil microemulsions and usually sodium bis(2-ethylhexyl)sulfosuccinate (AOT) is used as surfactant [6]. For instance cadmium sulfide nanoparticles can be prepared by mixing two different reverse microemulsions with aqueous phases containing either dissolved cadmium nitrate or sodium sulfide [6]. Coalescence of the micelles will lead to precipitation of insoluble cadmium sulfide while the particle size can be controlled by the water to surfactant ratio [6].

2.2 Nanoparticles and colloidal stability of nanoparticles

2.2.1 Nanoparticles

Particles and structures with a size of less than 100 nm are considered “nano” and often exhibit different properties than the bulk solid [11]. Nanoparticles are usually synthesized by chemical synthesis from atoms, ions and molecules also known as the bottom-up approach, whereas the top-down approach uses carving or etching to produce nanometer-sized structures, rather unsuitable to produce considerable amounts of nanoparticles [11]. The common characteristic of nanoparticles is their high surface to volume ratio, increasing the surface energy, their reactivity and also changing the ways it can react. For example a 10 nm particle contains around 15% surface atoms with different bonding, chemical environment and hence different properties than bulk atoms [11]. Since a high surface area is associated with higher energy, nanoparticles are very likely to agglomerate in order to reduce this energy and become thermodynamically more stable [1]. Moreover their absorption and scattering efficiency for visible light is reduced, giving them a transparent appearance [11].

2.2.2 DLVO theory

Derjaguin, Landau, Verwey and Overbeek discovered the DLVO theory describing colloidal stability by a combination of repulsive double layer forces and attractive van der Waals forces [6]. A good explanation model are two surfaces, separated by a distance ***D*** , which are able to hold an electrostatic charge and a solution in between containing the counterions [6]. Surface charge can originate from self - assembled layers of cationic or anionic surfactants, functional groups in polymers or inorganic material and is often pH dependent [1,6]. The surface of magnetite nanoparticles is usually negatively charged [1].

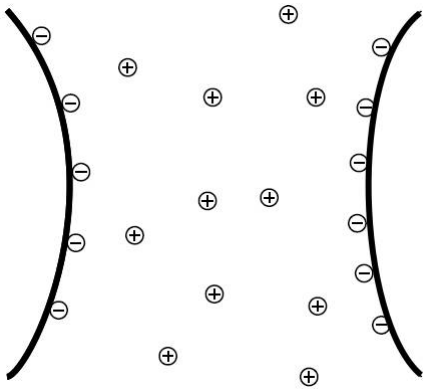

Figure 3 Simplified model of electrostatic repulsion

The double layer forces may origin from the electrostatic surface charge, but it's repulsive force comes from the entropically more favorable state of counterions being dissolved in between the surfaces. The solvent has a certain volume, creating an osmotic pressure and separating the two surfaces. Therefore the repulsive force in DLVO theory can be described as entropic force and highly depends on the ion concentration of the system. Salt addition reduces the entropy gain and dissolved counterions in between the surfaces create less osmotic pressure. The influence of salt can also be described as shielding the electric double layer forces and hence reducing colloidal stability. For instance at a $LiNO_3$ concentration of 10^{-4} M the force between two negatively charged mica surfaces is present at distances of more than 100 nm whereas at 10^{-1} M $LiNO_3$ the force will be limited to a few nm [6].

Van der Waals forces contain quantum mechanical dispersion interactions (London forces), thermally averaged dipole-dipole interaction (Keesom force) and dipole-induced-dipole interactions (Debye force). They are always attractive for the same material and are limited to distances below 10 nm, whereas the repulsive double layer force can be present at distances of more than 100 nm. If the distance between particles is high, they will repel each other, but once the double layer force is overcome, attractive Van der Waals forces will dominate and cause agglomeration [6]. For example 1 wt% silica nanoparticles in dispersion containing 3.5 wt% NaCl will segregate after 10 days, but at 2.0 wt% NaCl the dispersion is stable for the same time frame [12].

2.2.3 Steric stabilization

Steric stabilization is based on polymers adsorbed onto the surface. In case of particles, they then behave similar to polymers in solution and therefore are less sensitive to the salt concentration [4,6]. If the conditions (e.g. temperature, solvent) are right, the polymer chains dissolve and extend into solution creating repulsive entropic forces, which stabilize the particles against agglomeration [6]. Under those conditions the polymer chains prefer the contact with the solvent and a reduced distance between the particles would be accompanied by an unfavorable reduction of entropy [6]. On the other side, if conditions doesn't favor dissolution, the polymer chains prefer to be in contact with each other and agglomeration takes place. The transition is called Theta-point and knowledge about it is essential for understanding steric stabilization of particles in a certain polymer-solvent system [6].

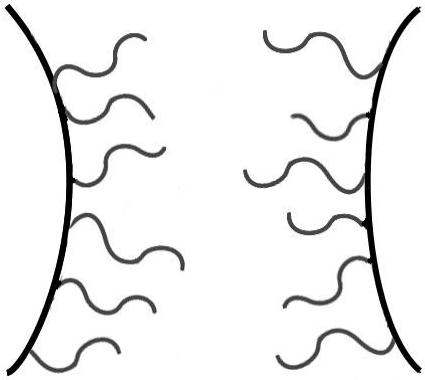

Figure 4 Simplified model of steric repulsion

In case of apolar solvents like toluene or hexane, particles will be stabilized by alkyl chains since they are soluble in these solvents. In case of polar solvents like water, the polymers described in paragraph 2.1.1 will provide steric stabilization [3]. Especially PEO is known to prevent protein and bio-molecule adsorption due to its completely non-ionic character [6]. However the discovery of specific antibodies against PEO after its use in medical treatment requires alternatives [7].

2.3 Magnetism and it's application in medicine

2.3.1 Superparamagnetism

Below the Curie temperature T_c bulk ferro- or ferrimagnetic materials contain regions of uniform magnetization known as domains (Weiss domains) with a material specific average size from 10 to 1000 nm [3,11]. In absence of an external magnetic field *H* those domains align randomly and cancel each other out in order to minimize the energy leading to no bulk magnetization. In the presence of an external magnetic field *H* alignment takes place, leading to overall magnetization [3] When all domains are aligned, saturation magnetization is reached [3]. After removal of the external magnetic field bulk ferro- or ferrimagnetic materials remain magnetized, because Weiss domains can't relax back completely due to friction between

the domain walls [3]. Hence there will be a difference between the applied magnetic field *H* and magnetization of the material, which is called hysteresis [1,3]. However in bulk paramagnetic materials also some alignment of magnetic moments takes place in the presence of an external magnetic field, but the effect is much weaker than in ferro- or ferrimagnetic materials and there isn't any hysteresis [11].

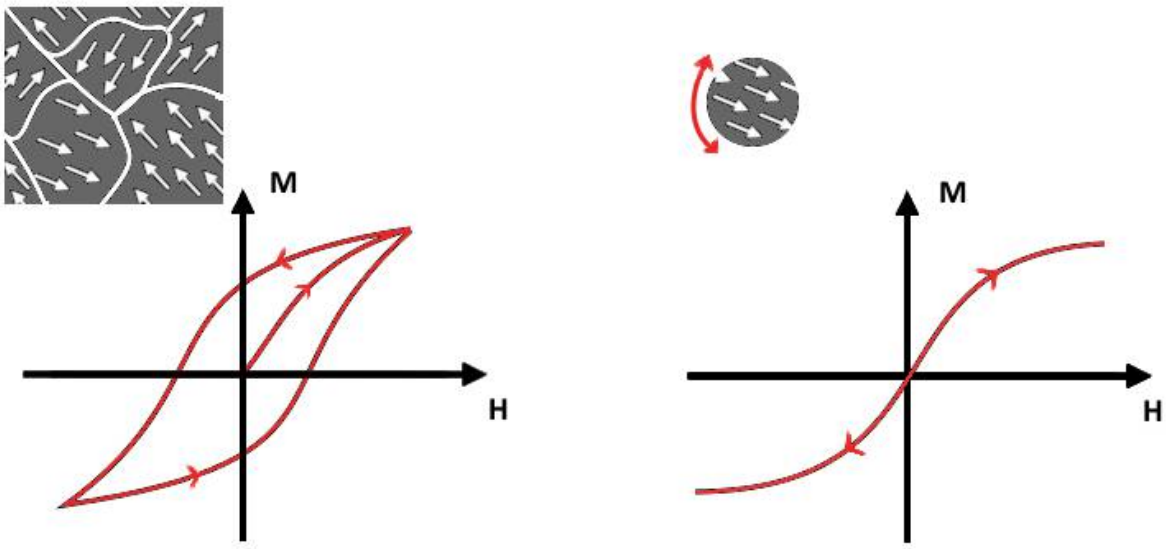

Figure 5 magnetization of bulk magnetic material (left); superparamagnetic behavior (right) [3]

When the particle size is smaller than one Weiss domain, the particles and their magnetic domains align with the external magnetic field *H*, but their magnetic orientation is not hindered by neighboring domains and the particles are free to relax or randomize after the external magnetic field *H* is removed [3]. Similar to paramagnetic materials there is no permanent magnetization or hysteresis, but the saturation magnetization can be as high as in ferro- or ferrimagnetic materials and therefore magnetic single domain particles are called superparamagnetic, [3,11]. The specific saturation magnetization σ_s of MNPs decreases with the particle size and is measured in emu g^{-1} [4].

2.3.2 Magnetic resonance imaging

Magnetic Resonance Imaging (MRI) is a based on the phenomenon of Nuclear Magnetic Resonance (NMR) and usually measures the ^{1}H density. Compared to other noninvasive imaging methods like Computer Tomography (CT) the contrast for soft tissue is higher and no ionizing radiation is utilized [13]. Under the influence of a static magnetic field the individual nuclear moments of nuclei like ^{1}H, ^{13}C, ^{19}F, ^{23}Na and ^{31}P tend to align parallel to the field, leading to a non-zero magnetization of the macroscopic sample. Those aligned nuclei gyrate at a certain angular frequency, proportional to the strength of the static magnetic field. If a perpendicular oscillating magnetic field of the same frequency hits the sample, their magnetization vector rotate to the transverse plain. NMR spectroscopy measures the frequency shift caused by the nuclei's chemical environment and can differentiate between ^{1}H in e.g water and fat [13].

After rotation to the transverse plain, the magnetization vector realigns or relaxes towards the static magnetic field and due to time-varying magnetization a voltage is induced into a coil. Two relaxation times are defined, which usually differ by one order of magnitude. T_1 describes the decay of magnetization parallel to the static magnetic field due to thermal fluctuations whereas T_2 describes the decay of magnetization transverse to the static magnetic field due to interaction with neighboring nuclei. The contrast in ^{1}H MRI is generated by the variation in relaxation times T_1 , T_2 and the proton density of the tissue. For example white matter in the brain has a T_1 of 790 ms and a T_2 of 92 ms whereas gray matter has a T_1 of 920 ms and a T_2 of 101 ms. Interesting for diagnosis is that malignant tissue can have longer relaxation times T_1 , T_2 [13].

2.3.3 Contrast agents

Hydrogen nuclei ^{1}H are not only used for *in vivo* MRI because they provide the best signal and contrast, moreover they allow facile enhancement of the image contrast by contrast agents. Since the relaxation times from hydrogen nuclei of water molecules are dependent on the surrounding media, contrast agents can indirectly affect T_1 and T_2 by interaction with those water molecules. Possible contrast agents are based on paramagnetic ions (e.g. Gd^{3+}, Mn^{2+}) or are susceptibility agents like superparamagnetic magnetite nanoparticles [13]. Gadolinium complexes like Gd-DTPA or Gd-DOTA contain a fast exchanging water molecule, which is responsible for shorter relaxation times T_1 , T_2 [13,14]. Further functionalization of the gadolinium complexes with neurotransmitters allows mapping of receptors on the neuron surface [13,14].

The presence of MNPs shortens the relaxation times T_1 , T_2 of hydrogen nuclei ^{1}H by interaction with surrounding water [15] and shows an even larger effect than paramagnetic ions [4]. Rhee et al. reported a linear correlation between the inverse of the relaxation times ($1/T_i$) and the concentration of MNP (approx. 7 nm) in solution [15]. The effect also depends on particle size, structure and present contaminants [4]. Larger MNPs exhibit higher magnetization and therefore have an bigger impact on the contrast [4]. Dextran coated magnetite nanoparticles were used to image the lymph-node system by non-specific accumulation and MNPs can be functionalized e.g. to target tumor cells or image neuronal activity [4,16].

2.3.4 Magnetic fluid hyperthermia

Magnetic fluid hyperthermia is the conversion of magnetic energy into thermal energy by superparamagnetic particles (e.g. magnetite nanoparticles) exposed to an alternating magnetic field [17]. Hosono et al reported a specific absorption rate of 15.7 W/g at 600 kHz by MNPs (13 nm) [17]. Since cancer cells are more sensitive to heat than normal cells [1,4], localized generation of heat has the potential to destroy cancer cells without the side effects of surgery, chemotherapy or radiotherapy [3,17]. Temperatures of 42-46°C cause death of cancer cells, but the heat generation shouldn't effect the healthy cells and MNPs have to be functionalized or targeted in order to selectively attach to cancer cells [4,17].

2.4 Magnetite and magnetite nanoparticles

Magnetite is Iron(II, III) oxide with the formula Fe_3O_4 and due to its ferrimagnetism it's the only natural occurring mineral with strong magnetism. In addition of being a common iron oxide mineral, magnetite crystals occur as well in biology (e.g. Magnetospirillum Magnetotacticum, bees, termites, birds), mainly for the purpose of magnetoreception, the ability to sense the earth's magnetic field [4]. Although humans lost this capability, their brain contains magnetite and they are able to metabolize it [3,4].

Magnetite and especially MNPs easily oxidize to maghemite (γ-Fe_2O_3) [1], which is cation deficient magnetite with the same crystal structure and ferrimagnetism below T_c. Magnetite has a density of 5.18 g cm^{-3} whereas maghemite has a slightly lower density of 4.87 g cm^{-3} [18]. Both materials contain hydroxyl groups on it's surface, which can react with bases as well as acids [18]. The isoelectric points of magnetite and maghemite are in between pH 6 and pH 7 [18]. Under basic conditions they are negatively charged whereas in acidic medium they are positively charged, but slowly dissolve in e.g. HCl [4,18].

Magnetite nanoparticles show superparamagnetic behavior below an estimated single-domain size of 128 nm [1]. The Curie temperature T_c for magnetite is 850 K and ranges from 820 K to 986 K for maghemite [18]. Bulk magnetite has a specific saturation magnetization σ_s of 92 - 100 emu g^{-1}, whereas the specific saturation magnetization of bulk maghemite is slightly lower at 60 - 80 emu g^{-1} [18]. The specific saturation magnetization of their nanoparticles increases with size and usually is in between 30 - 50 emu g^{-1} [1,4]. The presence of magnetic dipole-dipole attraction adds to the Van der Waals forces and therefore increases the demands on colloidal stabilization [4]. However Ferrofluids, “concentrated colloidal suspensions of superparamagnetic particles” [3], were already invented by Papell in 1965 and are commercially available today [1].

2.5 Synthesis of magnetite nanoparticles

2.5.1 Co-precipitation

Co-precipitation is probably the most simple way to produce magnetite nanoparticles [1]. A base is added to a solution of Fe(II)/Fe(III) with 1:2 ratio and the increasing pH leads to formation of magnetite according to following reaction [7], which usually is carried out under inert atmosphere due to air oxidation [1].

$$Fe^{2+} + 2\ Fe^{3+} + 8\ OH^- \rightarrow Fe_3O_4 + 4\ H_2O \quad (1)$$

The size of formed particles depends on temperature, pH, type of salts and it's concentration [1]. For instance Kurchania et al. synthesized MNPs with an average size of 13 nm by rapid addition of 10 mL ammonium hydroxide solution (25%) to a 175 mL solution of 2.15 g iron(II)-chloride and 5.8 g iron(III)-chloride (molar ratio 1:2) at 80°C [2]. The MNPs can be isolated by magnetic decantation, washing to pH 7 and drying in a vacuum oven at 60°C for 10 h [2].

Furthermore organic additives are useful for stabilization and size control of magnetite nanoparticles. For example aqueous solutions of polyvinyl alcohol (1 wt%) have stabilizing effects, trisodium citrate can be used to adjust the particle size and oleic acid can form surface complexes, influencing both stability and particle size [1].

2.5.2 Thermal decomposition

The synthesis of nanoparticles by thermal decomposition of organometallic compounds (e.g. metal acetylacetonates, carbonyls and metal fatty acid salts) allows good size and shape control, but requires temperatures of up to 300°C and long reaction times. It is carried out in organic solvents with high boiling point in the presence of stabilizing surfactants like fatty acid or oleic acid [1]. For instance, almost monodisperse MNP with a size from 3 to 50 nm, according to the reactivity and concentration of precursors, can be synthesized by thermal decomposition of a metal fatty acid salt, additional fatty acid and an activation agent in a hydrocarbon solvent at 300°C. This method yields nanoparticles dispersible in organic solvents. In order to prepare water-soluble magnetite nanoparticles, $FeCl_3$ and pyrrolidone are refluxed at 245°C for 1, 10 and 20 h yielding particles of respectively 4, 12 60 nm in size which can be further improved by addition of α,ω dicarboxyl- terminated poly(ethylene glycol) [1].

A similar process makes use of polyols like ethylene glycol or triethylene glycol, which serve as high boiling point solvents, reducing agents and stabilizers [19]. Therefore iron(III)-acetylacetonate and triethylene glycol were subsequently treated 30 min at 180°C and 30 min at 280°C yielding water-soluble spherical nanoparticles with narrow size distribution of around 7 nm [19].

2.5.3 Microemulsion

Inorganic nanoparticles can be synthesized by water-in-oil microemulsion, where reverse micelles are nano-reactors limiting the final particle size [1,3,5]. Magnetite particle formation occurs through recombination of reverse micelles in the oil phase or by diffusion of a hydrophilic base towards the reverse micelles trough the oil phase [5]. The nanoparticle size can be controlled by the water to oil ratio, but the formation of reverse micelles usually requires large amounts of organic solvent resulting in a low yield [1].

For instance, MNP with a fairly narrow size distribution of around 7 nm can be prepared in water/toluene microemulsion with Aerosol OT (sodium bis(2-ethylhexylsulfosuccinate) as surfactant. An aqueous solution of $FeCl_2$/$FeCl_3$ (1:2) is added to AOT/toluene in a ratio by weight of 1:8:15 and a similar microemulsion is prepared with a solution of tetramethylammonium hydroxide [5]. Combination of both microemulsions under sonication yields a black mixture from where the MNP can be recovered by precipitation with an excess acetone/methanol mixture [5].

2.5.4 Hydrothermal synthesis

Hydrothermal conditions require high pressure and temperature requiring Teflon lined stainless-steel autoclaves. The system inside the autoclave includes solid, liquid and solution phases, therefore the reaction depends on phase transfer and separation mechanism at the interfaces [1]. For instance, MNPs with a uniform size in between 9 and 12 nm can be synthesized by treating a mixture of iron salt, sodium carboxylic acid salt, carboxylic acid, ethanol and water at 160°C [1]. A similar approach produces monodisperse, hydrophilic ferrite spheres with tunable size from 200 - 800 nm by treating a mixture of iron(III)-chloride, ethylene glycol, sodium acetate and polyethylene glycol at 200°C for 8-72h. Ethylene glycol acts as reducing agent, whereas sodium acetate and polyethylene glycol prevent agglomeration [1].

2.6 Encapsulation and functionalization of magnetite nanoparticles

Further modification of MNP is crucial for their eventual application since they are easily oxidized or leached by acid and MNP dispersions have to be stable against agglomeration and precipitation in their final environment [1]. Usually inorganic or polymer encapsulation is necessary to protect the sensitive magnetite core against its environment, leading to a core-shell structure [1]. However controlled oxidation to maghemite can be useful in some cases and can be achieved by dispersing MNPs in acidic $Fe(NO_3)_3$ solution, stabilizing them in alkaline and acidic media while keeping some magnetic properties [1]. In case of *in vivo* application steric stabilization with hydrophilic, non-ionic, hydrogen bond acceptor polymers like polyethylene oxide is most efficient, because any protein adsorption will cause removal from the blood [4]. For more sophisticated medical applications like cancer treatment the polymer encapsulated MNPs have to be actively targeted. This requires conjugation of certain bio-molecules to the surface of the particles, which then can bind to corresponding receptors at the surface of certain cells [4].

2.6.1 Inorganic coatings

There is a variety of suitable inorganic materials for coating of MNPs like precious metals, silica or carbon. Gold has low reactivity and is easily functionalized with thiol groups, but the different lattice and surface properties of those materials cause difficulties [1]. A gold shell can be prepared by reduction of e.g. $HAuCl_4$ at the surface of MNPs [20], which can be carried out in reverse microemulsion directly after nanoparticle formation [1]. On the other side silica easily binds to an oxide surface like magnetite through hydroxyl groups, but it's not stable under basic conditions and pores weaken its barrier properties [1]. Silica surfaces are hydrophilic and also allow further functionalization [1]. Silica shells with adjustable thickness can be prepared by sol-gel processes with tetraethoxysilane (TEOS) and ammonia [1]. For instance, Xia et al. coated commercially available Ferrofluids in diluted solution by stepwise addition of ammonia and TEOS under continuous stirring, whereas the TEOS amount determines the shell thickness [1]. For better size control of the silica coating the hydrolysis of TEOS has to be carried out in reverse microemulsion [1].

2.6.2 Ligand encapsulation

The purpose of ligand encapsulation is mainly to increase the colloidal stability of MNPs by electrostatic or steric repulsion. For example Ferrofluids are “concentrated colloidal suspensions of superparamagnetic particles” [3] like oxalic acid capped MNPs, which are stable in oil phase [1,3]. Ligands with carboxylate groups like oxalic acid are anchored by coordinative and ionic bonds between the carboxylate anion and the iron cation. There is an equilibrium between anchored ligands and ligands in solution and if different ligands are present, ligands can exchange. It is useful to adjust the colloidal stabilization for different solvents, but in diluted solution, ligands will detach until an equilibrium concentration is reached. Since MNP dispersions are diluted by *in vivo* applications, ligands will be lost into solution and the particles agglomerate [3].

2.6.3 Polymer encapsulation

Polymer encapsulation protects the MNPs from oxygen, improve their colloidal stability and can tune their surface properties whereas especially bio-compatible polymers are promising candidates for medical applications [1,2]. In order to bind onto the surface of magnetite, the polymer has to contain functional groups like amino groups, ester groups, carboxylic acids or hydroxyl groups [1]. The difficulty is to carry out the polymerization or encapsulation before magnetic dipole-dipole attraction causes aggregation [1]. For instance, Kurchania et al. synthesized polyvinyl alcohol coated MNPs by dispersing them in PVAL solution for 12h at room temperature, which are then dried for 10 h under vacuum at 60°C [2]. Thermogravimetric analysis confirms the presence of PVAL, but TEM images only show large aggregates [2].

More sophisticated is the approach by Chu et al. , who reported three similar preparation methods for encapsulation of magnetite nanoparticles by an hydrophilic co-polymer synthesized from methacrylic acid (MA), hydroxyethyl methacrylate (HEMA) and the crosslinker N,N'-methylenebisacrylamide [5]. The first approach is seed precipitation polymerization of MA, HEMA and crosslinker in ethyl acetate initiated by AIBN at 55°C for 8 h, whereas the MNPs are dispersed in the organic solvent by sonication. The result is a polydisperse mix of encapsulated MNPs and larger particles with an average size of 200 nm [5]. The second approach is dispersing MNPs in water and forming a reverse microemulsion with AOT and toluene, which contains dissolved MA, HEMA and crosslinker. Polymerization is initiated by AIBN or potassium persulfate at 55°C [5]. The particles sizes are in between 80 - 320 nm and can be controlled by the water surfactant ratio [5]. The third approach differs to the second one only by adding the monomer and crosslinker directly to the water/AOT/toluene microemulsion used for the synthesis of MNPs as described in 2.5.3 [5]. This modification yields particles with an average hydrodynamic radius of 80 nm and improved particle size distribution [5]. The measured specific saturation magnetization of those polymer coated MNPs is 2.72 $\text{emu} \cdot \text{g}^{-1}$ and correlates to a magnetite content of 3.3 wt% [5], which is quite low for medical applications.

2.6.4 Targeted MNPs

Targeted MNPs are required for effective magnetic fluid hyperthermia or *in vivo* mapping of certain receptors [4]. MNPs can be targeted towards cancer cells by e.g. binding monoclonal antibodies (e.g. anti-HER2) onto their surface [4]. Akhtari et al. conducted *in vivo* studies with rats and reported MNPs with conjugated 2-deoxy glucose, which can cross the blood brain barrier and enhance the contrast for brain areas of increased activity [16].

2.7 Fenton's reagent

Fenton's reagent is the combination of an iron salt with Hydrogen peroxide creating hydroxyl radicals that can undergo many different reactions. For instance, it's an effective oxidant for organic compounds and gained attention for decomposing toxic waste like aromatic amines, dyestuff, pesticides and surfactants, however it's also useful in organic synthesis [21,22,23].

$$H_2O_2 + Fe^{2+} \rightarrow Fe^{3+} + HO^- + HO\cdot \qquad k_1 = 76 \tag{2}$$

$$HO\cdot + Fe^{2+} \rightarrow Fe^{3+} + HO^- \qquad k_2 = 3\cdot 10^8 \tag{3}$$

$$HO\cdot + RH \rightarrow R\cdot + H_2O \qquad k_3 = 10^7 - 10^{10} \tag{4}$$

The ratio k_3/k_2 describes the relative reactivity of organic compounds towards hydroxyl radicals whereas the addition to aromatics is very rapid. According to C. Walling alcohols like isobutanol with a triple-substituted group in β-position to the hydroxyl group, show the highest reactivity with a k_3/k_2 ratio more than 10, whereas ethanol and isopropanol show slightly lower reactivities. Ethers also show positive ratios similar to alcohols, but carbonyl compounds like acetone or acetic acid are unlikely to react with hydroxyl radicals. All in all the formation of stabilized radicals is favored, followed by oxidation, dimerization or reduction [21].

$$R\cdot + Fe^{3+} \rightarrow Fe^{2+} + \textit{oxidized product} \tag{5}$$

$$2\ R\cdot \rightarrow R-R \tag{6}$$

$$R\cdot + Fe^{2+} + H^+ \rightarrow Fe^{3+} + RH \tag{7}$$

Since some the presented reactions involve hydroxide ions or protons, Fenton's reagent is pH dependent. One should also consider the formation of iron hydroxides at neutral pH and it's ability for catalytic decomposition of hydrogen peroxide [24]. For efficient crosslinking the reaction conditions favors the dimerization. For instance tertiary butyl alcohol can be dimerized by Fenton's reagent in excess of sulfuric acid [22] and Bicak et al. observed the crosslinking of polyvinyl alcohol in the presence of Fenton's reagent under acidic conditions [25].

Another aspect of Fenton's reagent was investigated by Tolchev at al. [24]. They found a temperature and pH dependence on nano-sized iron oxide or hydroxide precipitates formed during Fenton's reaction [24]. Those precipitates are probably caused by hydroxyl ions, which are formed as a byproduct [24]. Under acidic conditions and ambient temperature ferrihydrites of 2-3 nm are formed, whereas direct magnetite formation only occurs above pH 8 and at elevated temperatures [24]. The temperature has a significant influence on the particle size of all observed precipitates, whereas higher temperature of up to 80°C leads to formation of bigger particles [24].

3 Chemicals and experimental procedure

3.1 Chemicals

- Polyvinyl alcohol (PVAL) 87-90% hydrolyzed (M_w=30300 g · mol^{-1} by viscosimetry; appendix 8.1)
- Polyvinyl alcohol (PVAL) 99-99.5% hydrolyzed (M_w=8170 g · mol^{-1} by GPC; appendix 8.2 - 8.4)
- $FeSO_4 \cdot 7\ H_2O$ (M=278.02 g · mol^{-1}) for analysis (Merk)
- H_2SO_4 20% prepared by dilution of sulfuric acid 96% (Sigma Aldrich)
- acetic acid (glacial) anhydrous 100% (Merk)
- n-Butanol 99% analytical reagent (LAB-SCAN)
- H_2O_2 30% (Merk EMPROVE (stabilized))
- Cetyltrimethylammoniumchloride (CTAC) 29% (Teqgard CETAC 29)
- sodium dodecyl sulfate (SDS)
- NH_3 26% (Sigma Aldrich)

3.2 Preparation of MNP

In a 250 mL erlenmeyer flask with magnetic stirrer 8.7 g of $FeSO_4 \cdot 7H_20$ (31 mmol) were dissolved in 20 mL distilled water. Subsequently 2 mL H_2SO_4 (20%) , 10 mL CTAC as the surfactant and 2 mL n - butanol as the co-surfactant were added. Alternatively CTAC can be replaced by different surfactants in similar molar amounts. Polyvinyl alcohol was dissolved separately in hot water at a mass concentration of 200 g · L^{-1} and added dropwise to obtain an almost transparent slightly cyan solution.

In order to carry out Fenton's reaction, hydrogen peroxide solution was added dropwise to this solution at room temperature or elevated temperatures of around 70°C. For oxidizing the right amount of Fe^{2+} 2.1 mL H_2O_2 (21 mmol) was necessary. The solution remained transparent and the color changed from cyan to dark brown or red. In order to obtain good MNP dispersions at the end, the iron ions embedded in PVAL were separated from the free iron ions in solution by salting out before ammonia addition. Therefore NaCl solution was added stepwise until a brown gel formed at the surface, which was collected with a spoon or filtered off and washed with distilled water. Sonication was useful to form bigger clumps facilitating separation. The PVAL precipitate re-dissolved easily in distilled water or a microemulsion mixture consisting of 20 mL H_2O, 10 mL CTAC and 2 mL n-butanol. More precipitate required more solvent, whereas re-dissolution difficulties were caused by too much salt addition and indissoluble residues were filtered off. The final step was addition of 5 mL ammonium hydroxide solution forming a dilutable viscous black liquid.

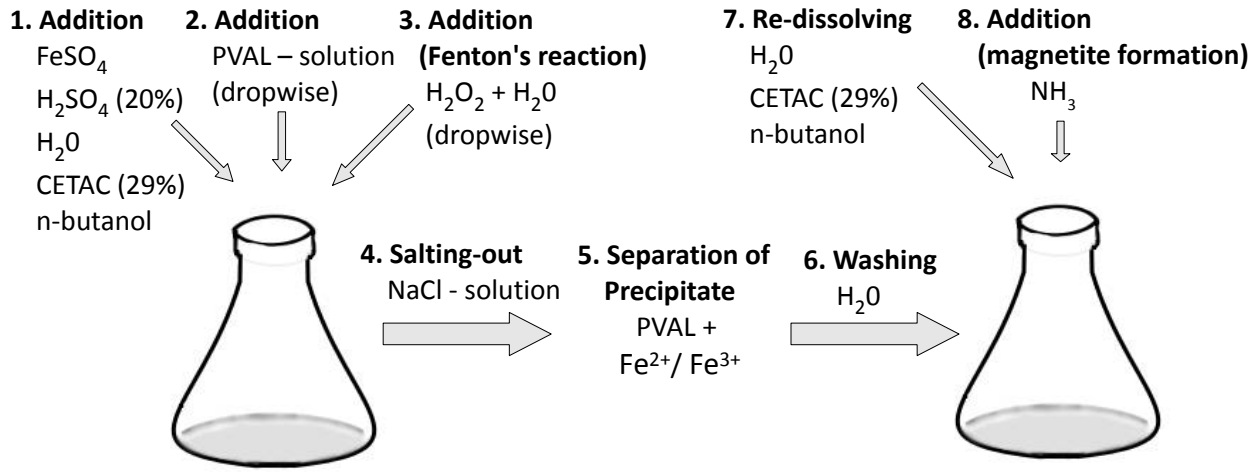

Table 1 Summary of varying recipes for preparation of MNP dispersions

Step	Chemical	standard	2 x PVAL	low CTAC	acetic acid	SDS	slow H_2O_2
1	$FeSO_4 \cdot 7H_20$	8.7 g (31 mmol)					
	H_2SO_4 (20%)	2 mL	2 mL	2 mL	-	2 mL	2 mL
	acetic acid (glacial)	-	-	-	1.4 mL	-	-
	H_20	20 mL					
	CTAC (29%)	10 mL	10 mL	10 mL	10 mL	-	10 mL
	SDS	-	-	-	-	3 g	-
	n-butanol	2 mL					
2	PVAL solution 200 g · L^{-1}	25 mL	50 mL	25 mL	25 mL	25 mL	25 mL
3	H_2O_2	2.1 mL + 5 mL H_20					2.1 mL + 20 mL H_20
4	NaCl solution	until precipitation					
5 + 6		separation of polymer and washing					
7	H_20	20 mL	70 mL	70 mL	20 mL	70 mL	70 mL
	CETAC (29%)	10 mL	10 mL	-	10 mL	-	-
	n-butanol	2 mL	2 mL	-	2 mL	-	-
8	NH3 (26%)	5 mL					

Concentrated MNP dispersions agglomerated and segregated within one or two days whereas more diluted samples were stable for at least some weeks. In difference to uncoated MNPs no rapid attachment to a magnet was observed, hence a normal magnetic stirrer could be used in all steps. Magnetism was estimated by placing a concentrated MNP dispersion in a petridish on a stirring plate, while at low speeds the surface will show the movements of the stirrer. To obtain a dry powder the concentrated dispersions had to segregate or were precipitated by acetone. Removal of surfactants and salt was ensured by washing with distilled water for at least 5 times. Eventual drying was carried out by leaching the precipitate in acetone for at least 12 h, pre-drying in a rotary evaporator and drying in a vacuum oven for at least 12 h at 60°C. The obtained brittle black clump was grinded to a powder exhibiting low magnetism.

3.3 Characterization methods

3.3.1 Dynamic light scattering (DLS)

DLS is a non-invasive technique to measure the size and the size distribution of nanoparticles [26]. It measures the intensity fluctuations of a laser beam after passing trough a dispersion of nanoparticles which undergo Brownian motion and scatter the laser light [26]. Small particles cause rapid fluctuations while bigger particles cause slower and larger fluctuations. For the computer program to calculate the particle size using the Stokes-Einstein relation, the exact viscosity has to be known [26]. In order to obtain the correct particle size distribution, high dilution of samples is necessary to correlate one laser intensity fluctuation to a single particle and not to several particles in a row.

For MNP dispersions obtained in this project, water dilutions of 1:100 or 1:200 were necessary, whereas macro-particles disturbed the measurement even at higher dilutions. Although filtering the samples in advance would have solved this problem, it would have influenced the final result and macro-particle formation had to be avoided during synthesis. Since the particle movement in dispersion depends on the viscosity it was measured beforehand with an Ubbelohe Viscosimeter for all 1:200 diluted samples confirming that the viscosity at such low concentration is identical to pure water. The refractive index of the dispersant is important and due to high dilution pure water (RI = 1.33) was assumed. The refractive index of the particle is only used to calculate the volume or number distribution and since no exact value for the particle RI was known, the evaluation of results has to focus on the intensity distribution. The measurement was carried out with a Malvern Instruments Zetasizer nano s at 25°C and processed by DTS nano software 4.0 . All sample were measured 5 times with at least 12 single runs.

3.3.2 Vibrating Sample Magnetometer (VSM)

A Vibrating sample magnetometer measures the voltage *U* induced to coils surrounding the mechanically vibrating sample while a magnetic field is applied. To relate the measured voltage to a certain magnetization, a reference with known saturation magnetization has to be measured beforehand.

According to literature nickel has a specific saturation magnetization σ_s of 55.1 emu · g^{-1} [27] and with following equations the specific magnetization can be calculated, whereas *k* is a constant and *m* the mass of the sample.

$$U = k \cdot m \cdot \sigma$$

$$\sigma = \sigma_{s,Ni} \cdot \frac{U \cdot m_{Ni}}{U_{Ni} \cdot m}$$

The reference sample containing 67.6 mg nickel induced 5687 mV at more than 6000 Oe. For actual measurement around 20 mg of dry powdered MNPs were pressed into a capsule of aluminium foil, because any loose particles would cause wrong results as they vibrate differently. This capsule was fastened inside the sample holder by a screw and the sample holder was mounted to the oscillator in a way that the sample was sourrounded by the coils identically to the reference measuremnt. A computer program recorded the magnetic field strengh and measured voltage.

3.3.3 Thermogravimetric analysis (TGA)

TGA records the sample weight while the temperature rises at a fixed rate and decomposition or dewatering will show up as weight loss of the sample [11]. In order to determine the iron oxide content of polymer encapsulated MNPs, the polymer had to be oxidized to carbon dioxide and water. The measurement was carried out with a Perkin Elmer TGA 7 under air flow of 20 mL · min^{-1} from 50°C to 600°C at 10°C per minute. Approximately 5-10 mg sample were filled in a aluminum capsule and mounted in the sample holder. The weight was recorded by Pyris Series computer program.

3.3.4 Transmission electron microscopy (TEM)

In TEM a high energy and high intensity electron beam passes trough the sample and trespassing electrons are detected giving a two dimensional projection of the sample [11]. In order to let any electron pass at all, the sample usually has to be a thin slice of less than 200 nm [11]. The electron beam requires vacuum and therefore the sample has to be dry, but nanoparticle dispersions can be directly dried on a copper grid with a thin layer of carbon, which is almost transparent to the electron beam. An Jeol TEM 1200 EX II electron microscope was used. The TEM samples were prepared by drying a few drops of 1:20 or 1:70 diluted aqueous dispersions at room temperature for two hours. The instrument was run at an acceleration voltage of 120 kV with a beam current of 90 µA. Images were taken by a camera software on a computer.

3.3.5 Photoelectron spectroscopy (ESCA/XPS)

In XPS the sample is subjected to X-rays liberating core or valence electrons up to a depth of up to 10 nm from the surface [18]. The kinetic energy of those electrons is related to the binding energy and their analysis gives information about elemental composition and bond characteristics [18]. The obtained spectrum shows the photoelectron intensity plotted against the binding energy in eV [18]. Different bonding of the elements is seen as small shifts in binding energy [18]. ESCA/XPS requires ultra high vacuum and therefore the samples had to be dried carefully [28].

3.3.6 Viscosimetry

Viscosimetry was done by an Ubbelohde viscosimeter, which is a simple glassware instrument combining an upper and lower liquid reservoir with a capillary in between. The time *t* for a certain volume (upper reservoir) to pass the capillary is measured which is proportional to the viscosity *η* [6]. Under dilute conditions, when the densities can be assumed identical, calculation of *η* only requires a calibration measurement with pure solvent (e.g. water) at identical temperature [6]. For molecular weight determination of water-soluble polymers by viscosimetry following equations are necessary [6].

Relative viscosity: $$\eta_{rel} = \frac{\eta}{\eta_0} = \frac{t}{t_0}$$

Specific viscosity: $$\eta_{sp} = \frac{\eta - \eta_0}{\eta_0}$$

Reduced viscosity: $$\eta_{\mathrm{red}} = \frac{\eta_{sp}}{c}$$

Intrinsic viscosity: $$[\eta] = \lim_{c \to 0} \frac{\eta_{sp}}{c}$$

The reduced viscosity is proportional to the polymer concentration and in a diagram measurements at different concentrations yield a straight line [6]. By extrapolating this line to zero the intrinsic viscosity is obtained, which only depends on the solvent, the polymer and its molecular weight [6]. The viscosity average molecular weight can be calculated by the Mark-Houwink equation [6].

$$[\eta] = KM_{\eta}^{\alpha}$$

The constants *K* and *α* are specific for a polymer and are usually found in literature [6]. In case of partially hydrolyzed PVAL they are reported by Masuelli [8]. The Viscosimetry was carried out in a water bath at 30°C and at least 3 measurements were combined.

4 Results and discussion

4.1 Fenton's reaction for synthesis of MNPs

Fenton's reaction has great potential to combine MNP formation and encapsulation in nearly one step, but it was a long way to obtain any MNP dispersion at all since only a small fraction of iron ions got entrapped within PVAL during Fenton's reaction. Consecutive ammonia addition led to formation of all kinds of magnetite particles or PVAL gels which agglomerated and segregated quite fast. Probably the affinity of PVAL towards the magnetite surface [2] causes gelation and agglomeration. A stable dispersion can only be obtained if there is just one kind of those particles. Therefore the PVAL with entrapped iron ions had to be separated before ammonia addition.

This paragraph will discus the preparation method based on observations in order to get dilutable nanoparticle dispersions. A nanoparticle dispersion should appear transparent, at least after dilution [11]. If Fenton's reaction already yields turbid dispersions the eventually obtained particles can't be nano-sized either. Moreover the final particle size is expected to be defined by Fenton's reaction since ammonia addition doesn't influence crosslinked PVAL.

4.1.1 Surfactant and microemulsion

The synthesis had to be carried out in a microemulsion with n-butanol as co-surfactant in order to solubilize all reactants, but it's unlikely that the Fenton's reaction occurred inside the micelles and that the micelle size had any influence on the particles. However surfactants might have been beneficial to prevent agglomeration during Fenton's reaction. CTAC as a cationic surfactant and SDS as anionic surfactant were used successfully yielding MNP dispersions. Cationic surfactants shouldn't have any advantage over other surfactant classes, since the particle surface ain't negatively charged magnetite [1]. However SDS has the disadvantage of precipitating at low temperature, which did occur during storage and non-ionic surfactants containing ethylene oxide groups precipitate at elevated temperature, which is unsuitable for Fenton's reaction. Some samples were also re-dissolved in microemulsion, but it had no significant influence on the stability of MNP dispersions.

4.1.2 Polymer solution

PVAL was dissolved separately in water by heating at 200 $g \cdot L^{-1}$ and this solution was added dropwise to the microemulsion salt mixture. Rapid combination of PVAL solution and concentrated salt solution usually led to salting-out of PVAL. 25 mL (5 g PVAL) and 50 mL (10 g PVAL) solution were used for the preparation of MNPs, whereas the molar amount of iron ions is 30 % and respectively 15 % of the PVAL repeating units. The prepared low-molecular weight PVAL was fully hydrolyzed and added in the same way. However the solution was still cloudy after heating at 80°C for more than one hour.

4.1.3 Acid and pH

The reaction was carried out at acidic conditions, because at neutral pH iron hydroxides form and catalytically decompose hydrogen peroxide [24]. The amount of H^+ should be equivalent to the OH^- formed by Fenton's reaction, however only approximate amounts were used, because the pH after reaction never exceeded 3 due to oxidation products. Amino acids have the potential to buffer the pH at 3, but no magnetic dispersions were obtained probably due to complex formation with Fe^{3+} ions

4.1.4 Hydrogen peroxide addition

The reaction was very fast and exothermic. A drop of hydrogen peroxide caused immediate color change from cyan over brownish and reddish to eventually dark red, indicating oxidation and nanoparticle formation. The different smell of the product could be caused by butyraldehyde and the final pH of 3, which was independent of the initial sulfuric acid addition indicates formation of carboxylic acid groups. Fast addition led to precipitation of crosslinked PVAL, whereas slow and diluted addition led to formation of visible polymer micro-particles with entrapped iron ions. Therefore hydrogen peroxide is best added dropwise and concentrated in order to obtain nanoparticles. Usually this was done at room temperature, but by placing the reaction flask in an oil or water bath the reaction was carried out at temperatures up to 80°C. According to Tolchev et al. the temperature can influence the size of iron hydroxide precipitates and hence the magnetite particle size [24].

An important aspect could be local pH increase by Fenton's reagent, which might form hydrated iron oxide clusters [24] entrapped within PVAL. The transparent appearance and dark red color after hydrogen peroxide addition indicated the presence of more than dissolved Fe^{3+} ions. Despite no magnetite is expected at this stage, different iron oxide nanoparticles were probably the precursors of the final MNPs. Since there was no certainty about the existence and composition of those precursor particles, the product after Fenton's reaction is referred as “PVAL with entrapped iron ions” or “PVAL encapsulated iron ions”.

4.1.5 Crosslinking of PVAL

According to reaction 2 highly reactive hydroxyl radicals were formed during Fenton's reaction, which can crosslink PVAL or oxidize organic compounds as described in 2.7 . Hydroxyl radicals abstract hydrogen most likely from the α-position and crosslinking occurs by dimerization of two radicals [25]. To verify the mechanism of PVAL crosslinking, isopropyl alcohol was treated with Fenton's reagent as a model compound since it has a secondary alcohol like PVAL. After extraction with ether and concentration a brownish liquid was obtained and slowly colorless crystals formed, whereas no volatile compounds were present anymore.

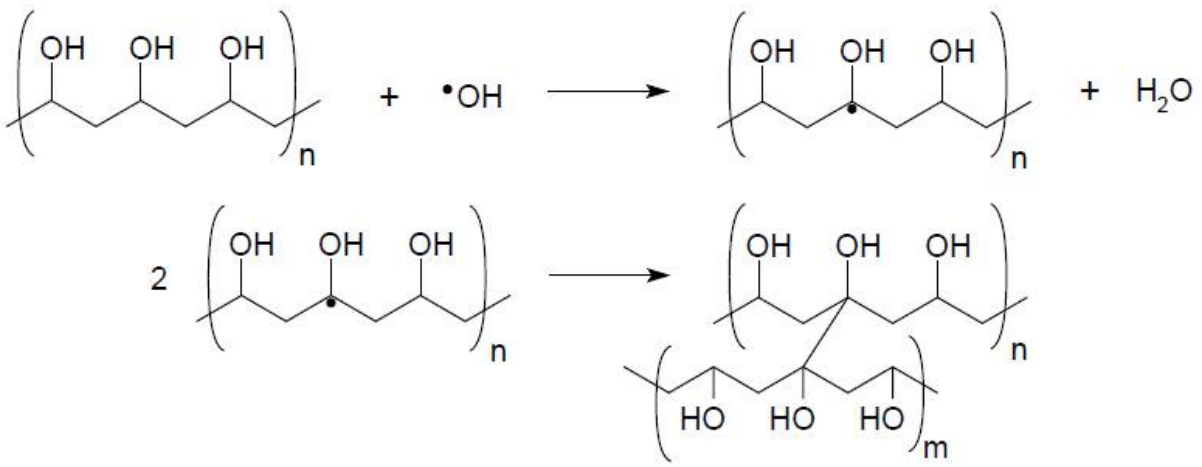

The NMR spectra (see appendix.) shows the presence of several possible dimerization and oxidation products and it's not possible to match certain compounds. However at 3,5 ppm and 4 ppm characteristic peaks of secondary hydroxyl group are present, representing non-volatile β-position dimerization products. Since α-position dimerization products cause no characteristic peaks in hydrogen NMR, they are expected to be present, too. In consequence PVAL crosslinking probably occurs unspecific at α- and β-positions. Whereas oxidation products are dominant in case of isopropyl alcohol, PVAL is less prone to oxidation due to less end-groups. Unfortunately no peaks with a shift of more than 10 ppm are present in the NMR spectra, which would represent carboxylic acids.

4.1.6 Separation of PVAL with entrapped iron ions

In order to eventually obtain stable MNP dispersions, the iron ions embedded in PVAL was separated from the free iron ions in solution by salting out before ammonia addition. The system was treated like a polymer solution, whereas the crosslinked PVAL has a higher molecular weight and according to theory, becomes insoluble first [6]. Concentrated NaCl solution was added stepwise until a brown gel forms at the surface, followed by separation with a spoon or filtering. Sonication was useful to form bigger clumps facilitating separation and the precipitate was washed with a small amount of water.

At standard procedure and partially hydrolyzed PVAL, this precipitate usually re-dissolved easily in distilled water or microemulsion mixture consisting of 20 mL H_2O, 10 mL CTAC and 2 mL n-butanol. Re-dissolution difficulties were caused by too much salt addition and required filtration of insoluble residues. Higher amounts of precipitate required more solvent. On the other side the fully hydrolyzed PVAL precipitated good by salting-out, but it didn't re-dissolve completely even under heating and CTAC addition. By using entirely fully hydrolyzed PVAL no black MNP dispersion could be obtained at all, whereas adding 20% of partially hydrolyzed PVAL stable MNP dispersion were obtained. This step already showed how much the preparation method depends on the polymer properties.

4.1.7 Magnetite formation

In difference to common co-precipitation methods the rate of ammonia addtion didn't seem to have any influence on the particle size and colloidal stability. Ammonia was added rapidly and concentrated under rapid stirring. When the system was too concentrated, ammonia addition caused gelation, but interestingly no irreversible agglomeration occurred and addition of water lead to the desired dispersion. Unlike uncoated MNPs no rapid attachment to a magnet was observed, hence a normal magnetic stirrer could be used in all steps. Instead the magnetism was tested by placing a MNP dispersion in a petridish on a stirring plate, while at low speeds the surface showed the movements of the stirrer. The sample should be stored in a closed bottle, because air slowly oxidizes the magnetite losing its magnetism, however in difference to other MNP preparation methods no protection atmosphere seemed to be necessary [1].

4.2 Prepared MNP dispersions

Table 2 List of analyzed magnetite nanoparticle dispersions

Nr.	Recipe	Comment
41	acetic acid	slow agglomeration
42	standard	slow agglomeration
43	standard	slow agglomeration
44	standard at 70°C	slow agglomeration ; darker appearance
46	2 x PVAL	more precipitate; no agglomeration but segregation
48	slow H_2O_2 at 80°C	partial agglomeration and segregation
49	slow H_2O_2 at 70°C	partial agglomeration and segregation
50	low CTAC at 70°C	no agglomeration or segregation
51	SDS at 70°C	no agglomeration or segregation
54	low CTAC at 80°C	no agglomeration or segregation
55	low CTAC at 70°C fully hydrolyzed PVAL	immediate agglomeration and segregation
56	low CTAC at 70°C 80% fully hydrolyzed PVAL + 20% partial hydrolyzed PVAL	partial agglomeration and segregation

Concentrated black dispersions obtained after ammonia addition are only stable for a short time, however slight dilution prevents agglomeration or segregation. Samples 41 to 44 are more concentrated and therefore agglomerated after one day, whereas samples 50 to 54 were prepared more diluted and were stable for the time frame of this project. However SDS containing sample 51 gelled during storage probably due to low temperature, but didn't segregate as samples 41 to 44. In difference to other samples, sample 46 segregated after some days but didn't aggregates and could be re-dispersed easily.

The stable dispersion of sample 50 has a dry weight of 7.3 % of which is a significant amount inorganic salt and after washing 4.2 wt % of polymer coated MNPs remain. Based on TGA results, approximately 20-30% of the dry weight is magnetite representing around 1 wt% of magnetite in the stable dispersions. This is more than twice as much as the (TMA)OH stabilized dispersions investigated by Dresco et al. [5].

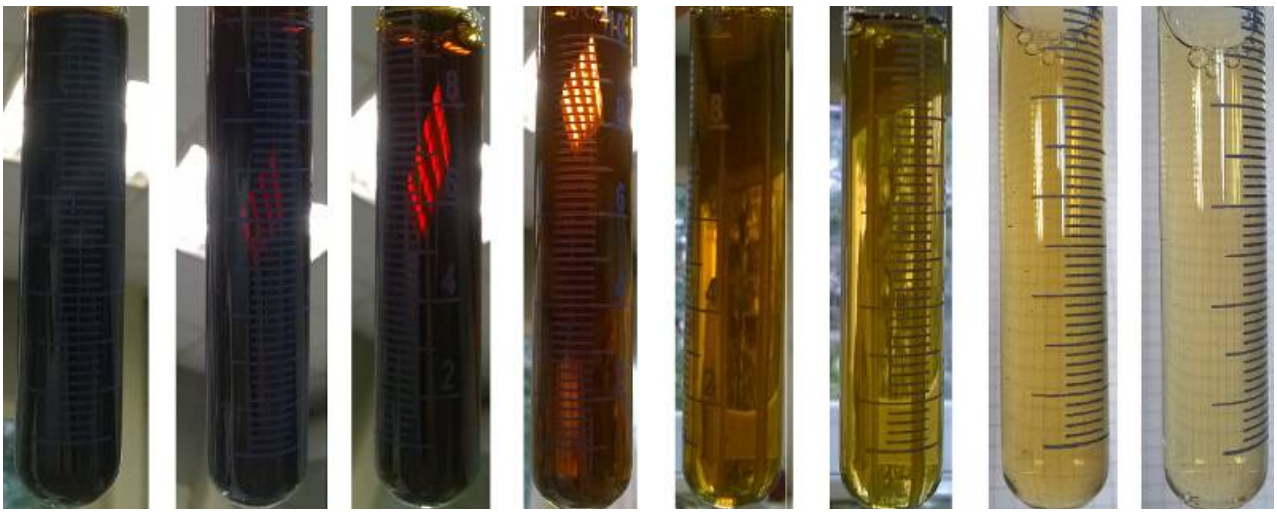

4.2 wt% 2.1 wt% 1.0 wt% 0.52 wt% 0.26 wt% 0.13 wt% 0.07 wt% 0.03 wt%

Figure 6 Images of sample 50 at different dilutions (wt% are given for polymer coated MNPs)

Drying the dispersions yielded mechanically stable films with embedded MNPs. The MNP content and optical appearance could be adjusted by mixing it with PVAL solution. Furthermore the dried dispersion partially re-dissolved again in hot water even in absence of a surfactant, indicating steric stabilization by partially hydrolyzed PVAL and the MNPs character as large polymer particles.

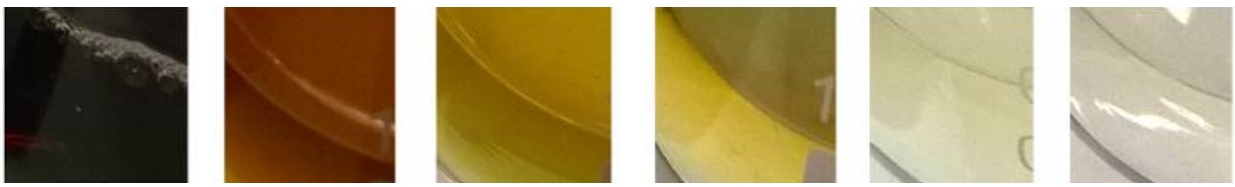

0 h 6 h 22 h 29 h 48 h 77 h

Figure 7 Coloration of sample 50 (1:10 diluted) in 0,1 mol HCl

For investigating the acid stability of MNP dispersions, 5mL of sample 50 were diluted 1:10 and set to pH 6 and followed by addition of 0.5 mL HCl at room temperature. Pictures were taken at different leaching times and show slow decoloration by leaching of MNPs. Since only a standard camera was used, no quantitative decoloration could be measured. The results show a complete decoloration after 3 days.

4.3 Particle size distribution

4.3.1 TEM results

At low magnification the polymer encapsulated MNPs were seen as a mottled structure adsorbed onto the smooth carbon grid, whereas all presented images were taken at a magnification of 200 k, due to best recognizance. The image contrast was enhanced by an image manipulation program (GIMP).

Sample 41 shows a broad particle size distribution from barely recognizable 1-3 nm to almost 15 nm. This could be related to the pH dependence as reported by Tolchev et al. [24], whereas acetic acid is less acidic than sulfuric acid. The smaller magnetite cores are certainly embedded into PVAL, whereas it's uncertain for the bigger magnetite cores. Moreover one polymer cluster seems to contain many magnetite cores or the polymer particles combine upon drying.

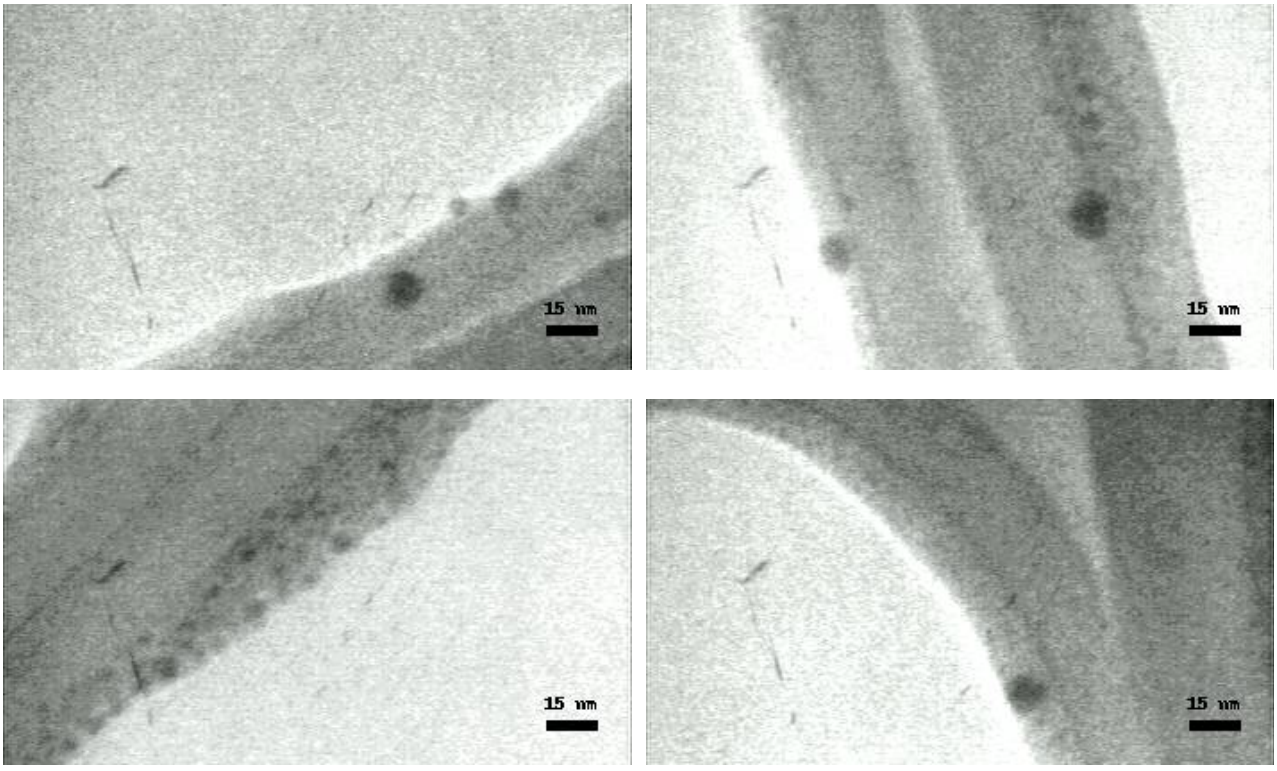

Figure 8 TEM images of sample 41 at 200k x

In sample 42 the majority of magnetite particles is with 1-3 nm very small and in difference to sample 41 no magnetite particles bigger than 7 nm were found. The image at 60 k is strongly contrast enhanced and therefore can't be compared to other pictures, but it might show the polymer shell. The polymeric particles are around 50 nm in size, containing several nano-sized magnetite cores indicated by small black spots.

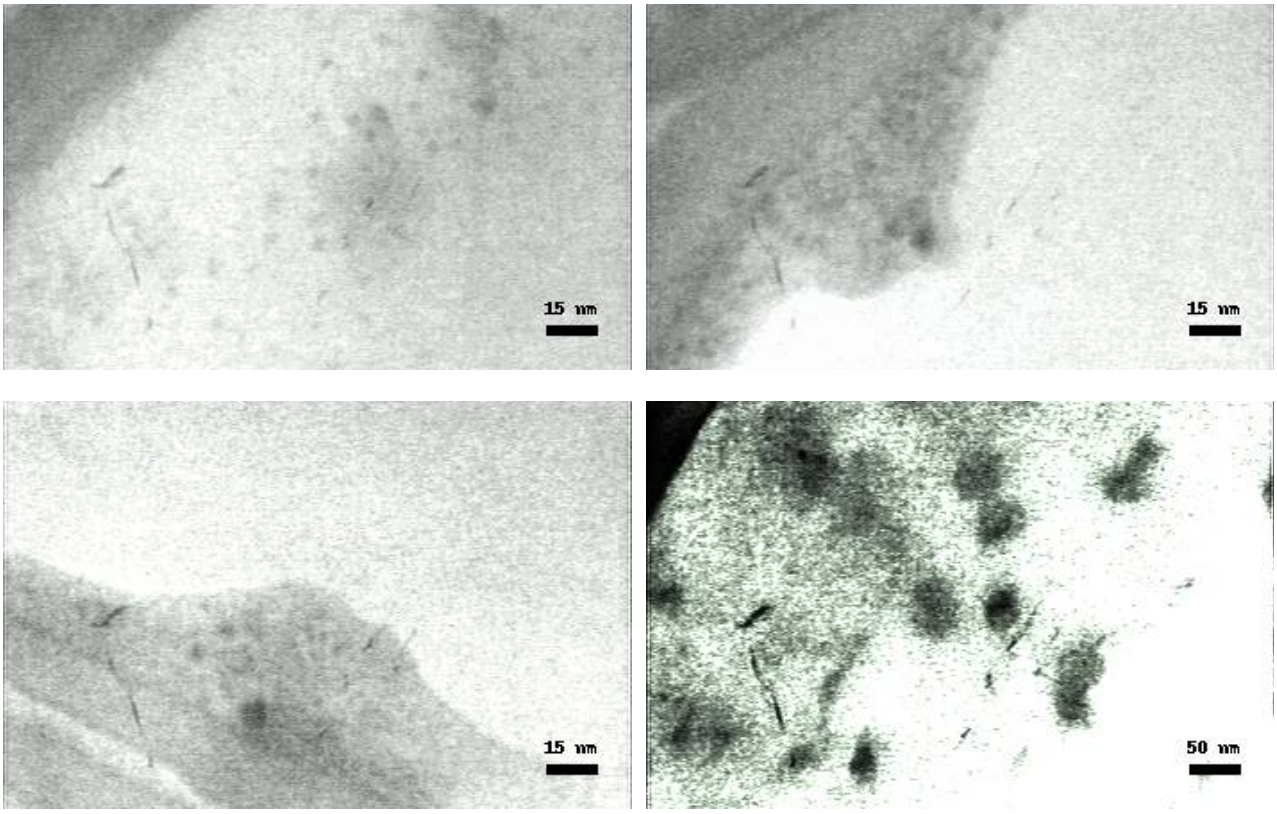

Figure 9 TEM images of sample 42 at 200k x and 60k x

The synthesis conditions of sample 43 were equal to sample 42, yielding magnetite cores of similar size. Accordingly only very small magnetite particles can be recognized within PVAL. Noticible in is the unregular shape of the polymer, which is either caused by drying or the the particles aren't spherical at all. However these pictures confirm that many magnetite cores can be embedded in one polymer particle.

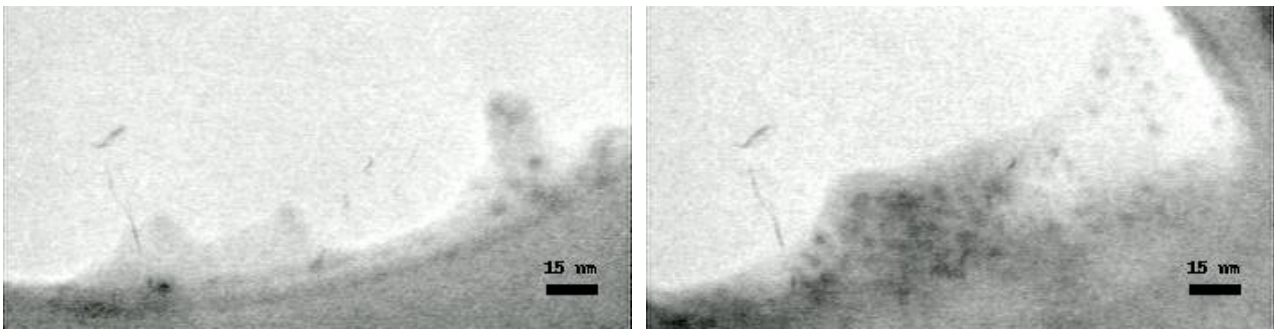

Figure 10 TEM images of sample 43 at 200k x

In difference to previous samples, sample 44 shows recognizable magnetite cores in between 5-10 nm, despite the presence of some smaller magnetite cores. As well as the pH dependence seen in sample 41, sample 44 corresponds to the temperature dependence reported by Tolchev et al. [24], whereas higher temperature leads to bigger particles. In the upper right picture one magnetite particle seems to be surrounded by a material of lower contrast as indicated by a convexity around it, but in general it's difficult to recognize the polymer due to its low contrast.

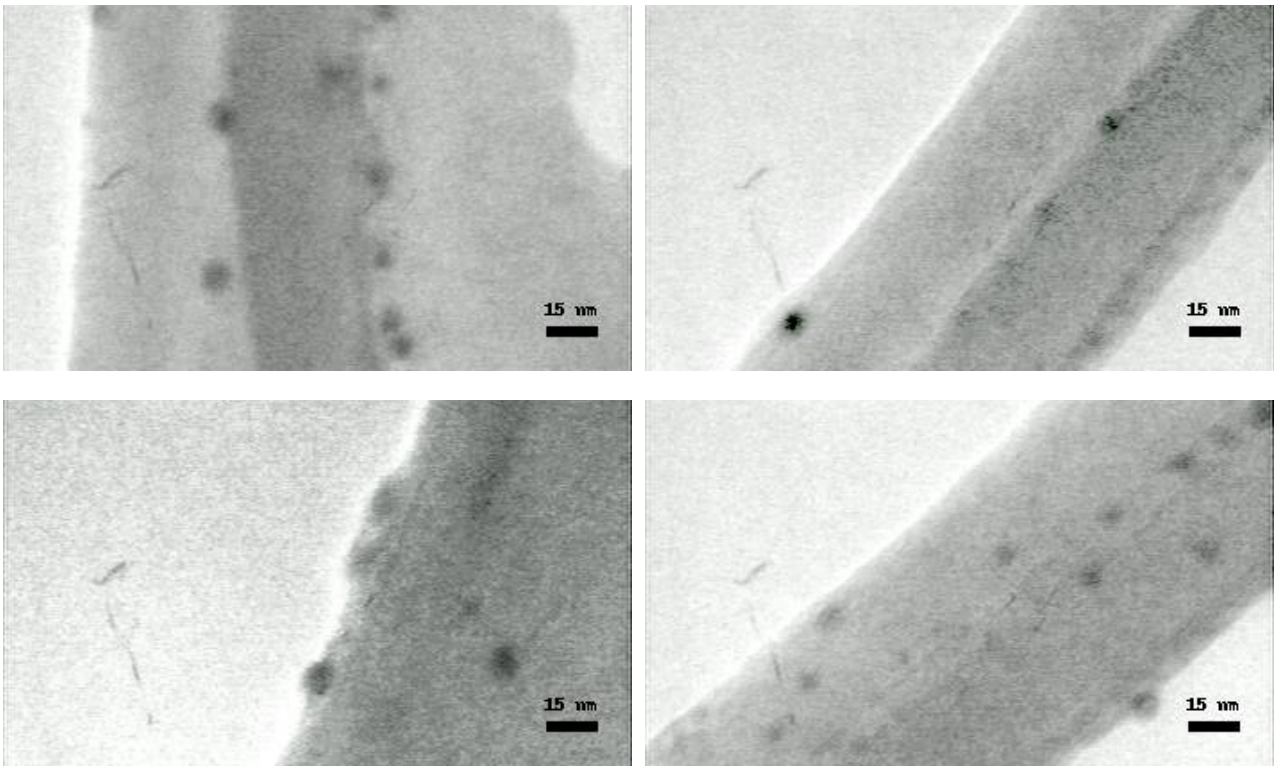

Figure 11 TEM images of sample 44 at 200k x

Unlike other samples, it's difficult to recognize any magnetite cores in sample 46 at all. In the left picture 3 magnetite cores can be identified, but they seem partially hidden by polymer. Although the right picture doesn't show any cores, a grainy texture indicates small magnetite cores as in sample 42 and 43.

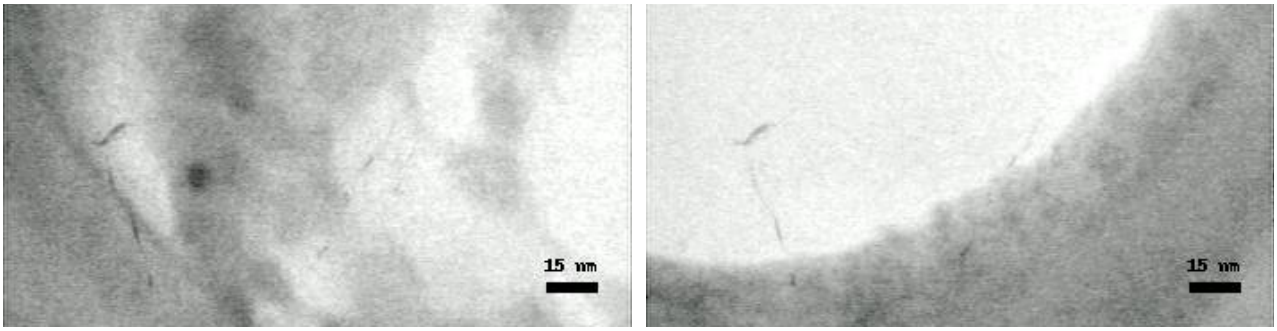

Figure 12 TEM images of sample 46 at 200k x

TEM images show magnetite cores of around 10 nm only for synthesis at elevated temperature or with acetic acid, which correlates to the results of Tolchev et al. [24]. TEM can't give representative magnetite core size averages, but the polydispersity seems to be quite high even no magnetite cores larger than 15 nm were observed. It was not possible to determine the particle size distribution including the polymer shell, though it is possible to identify the polymer shell in some cases. The size of the overall particles including the polymer shell was measured by DLS.

4.3.2 DLS results

In difference to TEM, DLS measures the size of the whole particles including the polymer shell and yields representative particles size averages as well as the particle size distribution. Measurements confirm the presence of nanoparticles, whereas all samples show an hydrodynamic radius of more than 20 nm and an high particle size distribution. Since sample 42 represents the standard receipt and has only one peak in the nanometer range it will be the reference for comparison.

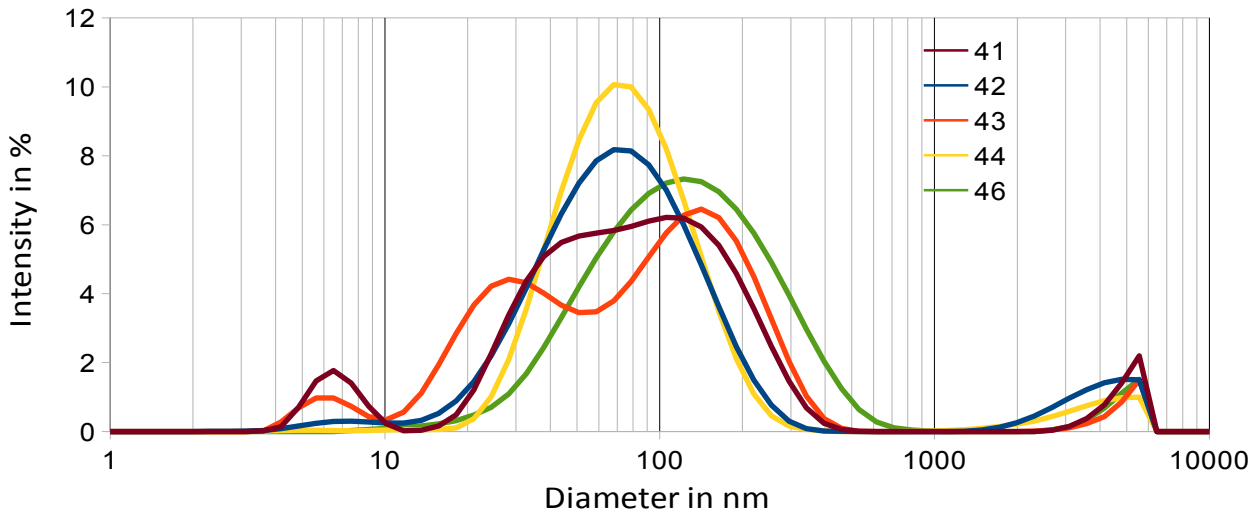

Figure 13: Intensity distribution of the particle sizes

Sample 42 and 43 were prepared by the same receipt, but already a slightly different color of 1:20 diluted dispersion indicated a different outcome. Whereas sample 42 only has one peak with an z-average of 68 nm and a polydispersity index (PDI) of 0.445 , sample 43 shows 3 peaks with a PDI of 0.712 . The first peak at around 6 nm is to small to represent core-shell MNPs. More likely is the presence of non-encapsulated MNP due to insufficient washing of the polymer precipitate before ammonia addition or PVAL nanoparticles without any magnetite core. Quite unlikely should be the presence of surfactant micelles at such high dilutions. The double peak of sample 43 is in the same range as the single peak of sample 42 and probably represents two different groups of encapsulated MNPs. One reason could have been the hydrogen peroxide addition rate, which wasn't necessarily kept constant. An adjustment during the reaction could have caused

two different products. As experienced for other samples, fast addition of hydrogen peroxide caused formation of visible PVAL micro-particles. In this case the crosslinking was faster than the diffusion or mechanical stirring of reaction mixture. Another reason could be the stirring rate itself, which wasn't controlled either and might have been adjusted during reaction.

Sample 41 was synthesized with acetic acid and the particle size distribution is broader than in sample 42, but more narrow than in sample 43. Although TEM shows a varying size of magnetite cores, the size variety of polymeric particles is less than in sample 43. Therefore the size of the magnetite core and the thickness of the polymer shell is expected to be independent of each other. The same accounts for sample 44, which is much darker at a dilution of 1:20 than sample 42, but has a similar average particle size of 66 nm and a even narrower PDI of 0.318 . A possible explanation could be the lower viscosity and faster diffusion of reactants at higher temperature, which decreased the influence of mechanical stirring. The doubled amount of PVAL in sample 46 caused an increased particle size with an z-average of 99 nm. Although the yield increased at higher concentration of PVAL, it probably caused the increased particle size, too.

The major difference of the second set of samples towards the first was an higher dilution, yielding a stable dispersion and no more surfactant addition before the final step. However the 1:100 diluted samples for DLS measurement weren't prepared immediately after MNPs synthesis and slight unnoticeable aggregation might have occurred. As a result of less stabilizing surfactant and a longer time before DLS sample preparation, the average particle size increased from 66 nm in sample 44 to 112 nm for sample 50 while the other synthesis parameters were identical.

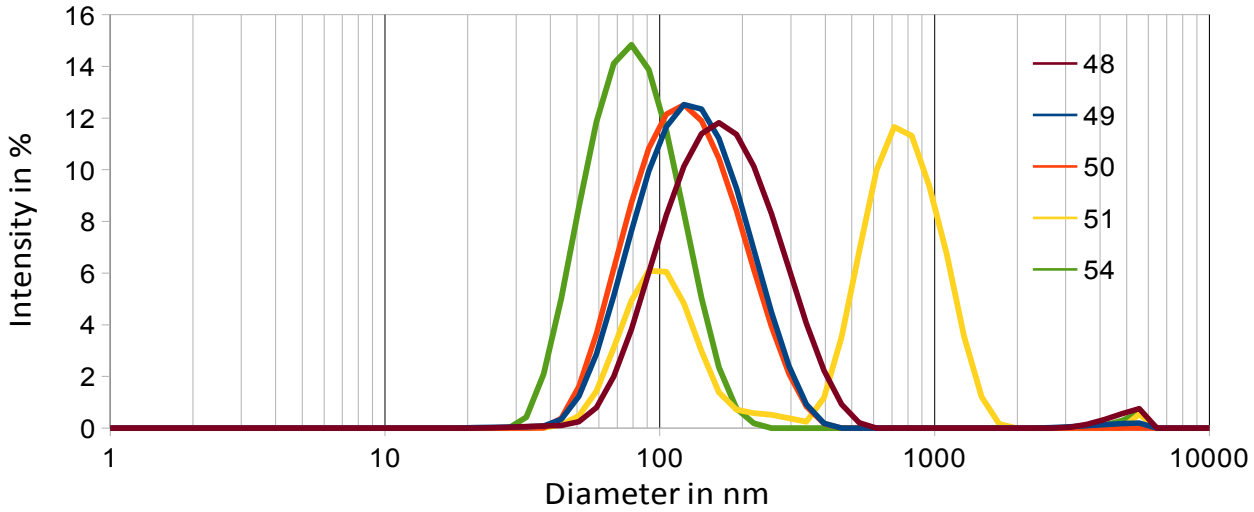

Figure 14: Intensity distribution of the particle sizes

Despite the increased particle size, the second set of samples shows a lower PDI from 0.186 to 0.229, whereas sample 51 is an exception, due to instability during storage. Its one peak at 100 nm is similar to the other samples indicating equal suitability of SDS for MNP synthesis, but a second peak at 600-1000 nm and colorless particles probably represents precipitated SDS and non-crosslinked PVAL at low storage temperatures. It might be disadvantageous in this case, but it reveals a possible procedure to remove surfactant residues from the final product.

Figure 15 compares the size of nanoparticles from sample 50 after acid leaching and re-dissolving of dried dispersion to the original MNPs. In difference to the colloidal stability discussed in previous paragraphs these DLS results give information about the stability of the nanoparticles and their encapsulation. The acid leaching (Figure 7) leads to a colorless solution, indicating complete dissolution of iron oxides. As already mentioned addition of sodium chloride leads to salting out of polymer, however the polyvinyl alcohol is crosslinked and not completely dissolved. According to DLS results two different PVAL cluster sizes are present in the colorless dispersion. Whereas random disintegration of MNPs should yield a broad size distribution of PVAL clusters, the DLS measurement shows two separate peaks. Whereas one is in the size range of the original particles before acid leaching, the other peak is around 10-20 nm. The question is if those two peaks represent two different sizes of PVAL clusters or one kind generating two different signals. Even if the PVAL is crosslinked sufficient enough, protons will diffuse inside and dissolve the iron oxide core, but the encapsulation would remain intact. Those hollow PVAL clusters are probably swollen and slightly larger than the original particles, but might generate different signals since the laser beam is not absorbed by a core and wouldn't be scattered at certain angles.

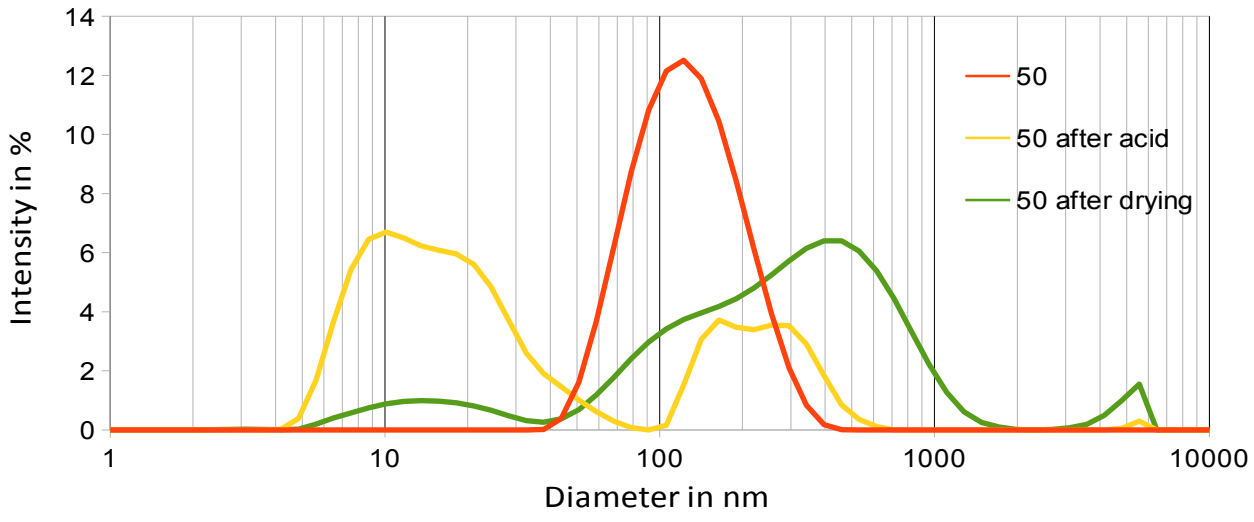

Figure 15: Intensity distribution of the particle sizes

For the MNPs after drying the picture is different. Broad peaks and particle size distributions indicate all kinds of agglomerates and even some smaller fragments of the original particles. Only a small fraction of the original particles is recovered, while most of it remains as 200-1000 nm agglomerates some particles. Maybe surfactant addition and sonication could reduce the size of agglomerates, but disintegration would increase, too. Hence the original particle size distribution can't be re-obtained after drying and any functionalization or modification step has to be carried out with the original aqueous MNP dispersion.

Samples 55 and 56 were prepared with fully hydrolyzed PVAL of lower molecular weight. Since re-dissolution of precipitate in sample 55 caused difficulties, sample 56 contains 20% partially hydrolyzed PVAL with higher molecular weight. Moreover immediate agglomeration and segregation took place in sample 55 and only the remaining red dispersion, which probably doesn't contain any magnetite, could be diluted and analyzed with DLS. The sample 56 precipitate refers to a stepwise salting-out with sodium chloride. After separating the first precipitate a second portion of sodium chloride was added and more PVAL with embedded iron ions precipitated. According to its optical appearance the first precipitate was similar to samples 41 to 54 and the second precipitate was similar to sample 55. In consequence partially hydrolyzed PVAL of higher molecular weight is more sensitive to salting-out but easily re-dissolves. Both samples 55 and 56 show two peaks, except they are separated into two samples in the latter case. The first peak is in the size range of the other samples, representing encapsulated MNPs, but the second peak ranges from several hundred nanometers to a few micrometers. Random agglomeration of MNPs should yield a broad size distribution similar to sample 50 after drying and re-dissolving, but the peaks are rather narrow like the second peak of sample 51. Therefore this second peak might be caused by undissolved PVAL particles. In both cases the polymer solution wasn't completely transparent before addition, despite long dissolution times close to the boiling point.

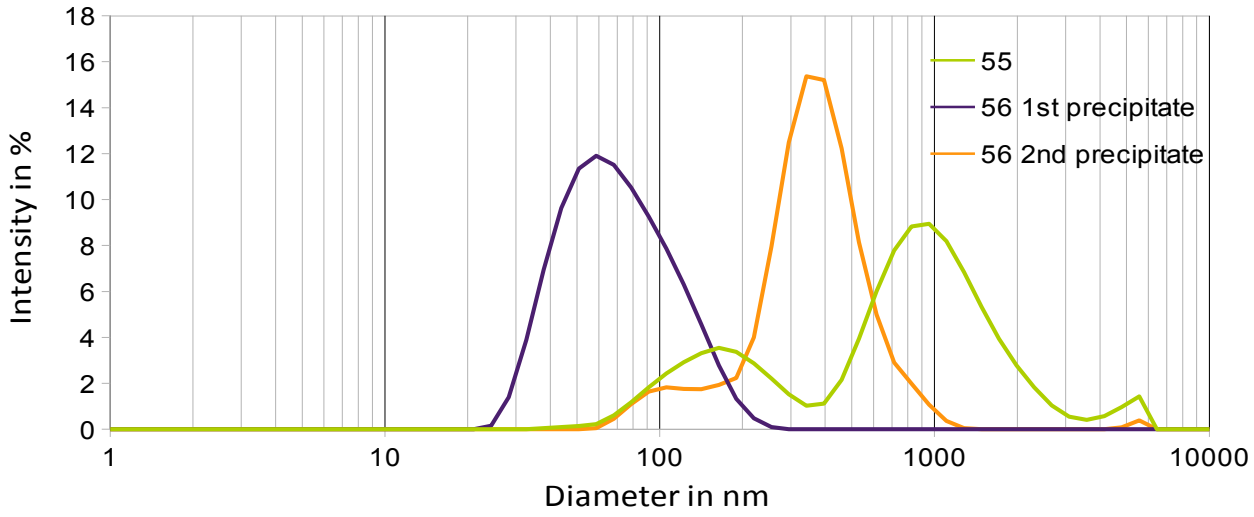

Figure 16: Intensity distribution of the particle sizes

In conclusion the pH and temperature influences the size of magnetite cores as reported by Tolchev et al. [24] and the polymer concentration and properties influence the size of the overall particles with the polymer shell. The attempt to decrease the particle size by using fully hydrolyzed PVAL of low molecular weight wasn't successful, because of dissolution difficulties before and during the synthesis of MNPs. The surfactant has a small impact on the particle size and probably just slows down aggregation of MNPs in the final dispersion. According to the intensity distribution most samples contain a small amount of micro-particles, which are either formed by crosslinking during Fenton's reaction or originating from the raw materials. Since microfiltration should be carried out before final *in vivo* application, a small amount of micro-particles would be easy to remove.

4.4 TGA results

The residues of sample 42 were red and quickly attached to a stainless-steel spoon, which was due to their magnetism or electrostatic charge. The same wasn't observed for other samples, whereas white particles in sample 44 before and after TGA measurement indicate a high amount of salt contamination which certainly decrease its magnetism.

Table 3 Summary of TGA results

sample	residues in %
42	29.5
43	19.9
44	25.5
46	29.9

The decomposition occurs in two steps and the samples reached a steady weight at 600°C. The polymer content was determined, whereas the weight loss probably includes a small portion of water or organic low molecular weight compounds. The polymer content is about 70-80% and can be found for each sample in Table 3. However the residues contain a significant amount of inorganic salt and therefore the magnetite or maghemite content can't be quantified correctly. By combining the results of TGA and ESCA it will be possible to compare the samples with each other, but still no numbers can be given, because ESCA is only sensitive towards the surface and doesn't recognize the iron oxide cores.

4.5 Elemental analysis by ESCA/XPS

Two different information were obtained from ESCA analysis, first the elemental surface composition of the dried particles by survey spectra and second the bonding of carbon atoms by carbon spectra. In difference to TGA only the surface is analyzed and results can't be compared directly.

Table 4 Atomic concentrations in %

Sample	**C**	**O**	**Na**	**S**	**Cl**	**Fe**
42	50.61	30.38	9.9	1.56	6.96	0.59
43	56.25	33.29	5.79	1.67	2.25	0.75
44	43.4	35.68	12.54	3.84	4.54	-
46	35.69	31.94	17.96	2.39	11.65	0.37

The survey spectra doesn't show any iron at all in sample 44, whereas in the other three samples traces of iron could be detected. On the other side the PVAL encapsulated MNPs studied by Kurchania et al. show an atomic concentration of iron similar to uncoated particles [2], but the polymer content of those particles is less than 20 wt% [2]. The small iron signal is an indication for good encapsulation of magnetite particles since the actual iron oxide content is in the range of 20% according to TGA.

Tabelle 5 Calculations based on atomic concentrations

Sample	$O-SO_4^{2-}$	$\frac{C}{O-SO_4^{2-}}$	$\frac{Na}{Cl+SO_4^{2-}}$	inorganic wt%
42	24.14	2.1	0.98	39.9 %
43	26.61	2.11	1.04	27.3 %
44	20.32	2.14	1.03	49.3 %
46	22.38	1.59	1.09	58.3 %

In theory PVAL has a carbon to oxygen ratio of 2:1, which is independent from the degree of hydrolysis. Carbon contamination is common, but three samples show a similar ratio, close to the theoretical ratio, unlikely caused by random contamination. Samples 42, 43 and 44 have in common, that slightly more carbon is present than expected indicating either a loss of hydroxyl groups or a contamination with alkyl chains during the synthesis. For instance n-butanol was used as co-surfactant, whereas hydroxyl radicals could have caused addition to the polymer chain or vacuum drying was insufficient for its removal. On the

other side Sample 46 shows a significant higher amount of oxygen. A source for this higher oxygen ratio could be water, either due to insufficient drying or as crystal water in sodium sulfate.

All samples contain a significant amount of inorganic salt on its surface, which is either sodium chloride or sodium sulfate as the ratio of sodium ions to these anions is nearly one. The weight of chloride and sulfate atoms is much higher than carbon and oxygen causing this high wt%. Moreover there is a large variations in between these samples probably due to different precipitation or segregation before drying.

Tabelle 6 Summary of carbon spectras

			42	43	44	46
Band	Position	Shift		Area %		
1	283.5	0	54.5	54.1	62.8	57.8
2	285	1.5	41.8	40.4	30.1	34.8
3	286.5	3	3.7	5.5	3.7	4.8
4	287.5	4	0	0	3.5	2.6

The reference position of the C-C bond is at 284.8 eV [28] and hence there is an offset of approximately 1 eV in present spectra. More important is the shift of the other peaks, which is independent from the instrument offset. A shift of 1.5 eV is caused by an C-O bond and is expected to represent the hydroxyl groups of PVAL [28]. A shift of 4 eV usually represents carbonyl or carboxyl groups [28], which could also be responsible for a shift of 3 eV since the the peaks are rather small and difficult to isolate. Carboxyl groups could be caused by the oxidizing environment of Fenton's reagent or origin from contamination. According to literature PVAL should show two similar carbon peaks since every second carbon contains an hydroxyl group [29], but the C-C peak is slightly larger than the C-O peak. It is difficult to say whether this inequality is caused by different instrument signal, contamination with alkyl chains or loss of hydroxyl groups by Fenton's reaction.

4.6 Magnetization

All four samples are superparamagnetic with no hysteresis, but the specific saturation magnetization σ_s differs quite much. The divergence of samples 42, 43 and 44 can be explained by different magnetite contents, whereas the magnetization of sample 46 decreases at high fields, probably caused by diamagnetic contribution from water [5]. In correlation with this, ESCA results of sample 46 show an increased oxygen ratio probably caused by water.

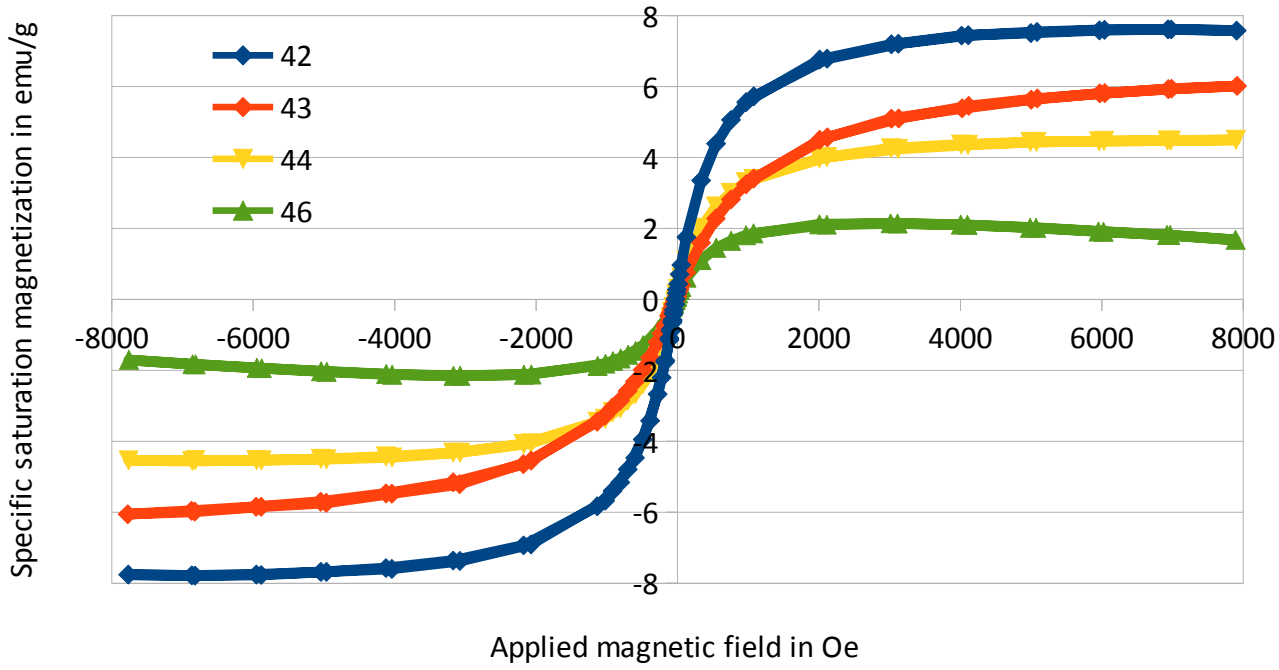

Figure 17 Specific magnetization of polymer coated MNPs

Taking in account the polymer content determined by TGA and inorganic salt contaminants determined by ESCA, the specific saturation magnetization for samples 42, 43 and 44 would be around 30 emu g^{-1} , which correlates well with partially oxidized MNPs. Sample 42 has a lower polymer content and low salt contamination, sample 43 has the lowest salt contamination but a high polymer content and sample 44 has high polymer content and much salt contamination. The VSM measurements leave no doubt about the desired super-paramagnetism of prepared MNPs, but it's difficult to present representative numbers for the specific saturation magnetization since inorganic salt contamination can't be quantified.

5 Conclusion

The developed preparation method combines MNP formation and direct encapsulation within polyvinyl alcohol (PVAL) by using Fenton's reagent. In general Fenton's reagent is the addition of hydrogen peroxide to a solution of Fe^{2+} , causing the formation of Fe^{3+} , hydroxyl radicals and hydroxyl anions [24]. At the right Fe^{2+}/Fe^{3+} ratio magnetite will form eventually, hydroxyl radicals can crosslink PVAL and hydroxyl anions are probably the cause for nano-sized iron hydroxide precipitates as reported by Tolchev at al. [24]. After separating the PVAL with entrapped iron ions from the reaction mixture by salting out, the polymeric precipitate easily re-dissolves in distilled water and ammonia addition leads to formation of magnetite nanoparticle (MNP) dispersions.

Dispersions containing around 4 wt % polymer coated MNPs showed no visible agglomeration during the time frame of this project, whereas more concentrated dispersions agglomerated and segregated within a

few days. The particles itself have a size of around 100 nm according to DLS measurements, which is much larger than the desired size of 20 nm, but TEM images reveal magnetite cores no bigger than 15 nm. TGA data shows inorganic weight contents of 20-30%, including salt contamination as revealed by ESCA. Moreover ESCA detected only traces of iron oxide in the surface layer indicating nearly complete encapsulation by PVAL. Magnetization measurements confirm expected superparamagnetism with no hysteresis. Therefore it should be possible to obtain desired magnetite nanoparticles by improving this method.

An increased polymer content during reaction increases the yield, but obtained particles have a larger hydrodynamic radius and show lower magnetization, despite identical size of magnetite cores. An increased temperature or pH leads to bigger magnetite cores of around 10 nm, while at room temperature the average core size is below 5 nm. Therefore the size of the magnetite core and the hydrodynamic radius of the polymer shell are expected to be independent. The pH and temperature influence the size of magnetite cores as reported by Tolchev et al. [24], whereas the polymer concentration and properties influence the size of the polymer shell and its steric stabilization. In order to decrease the particle size, PVAL with lower molecular weight was prepared by RAFT polymerization of vinyl acetate followed by methanolysis yielding fully hydrolyzed PVAL. However fully hydrolyzed PVAL doesn't dissolve sufficiently and provides only weak steric stabilization due to strong intermolecular hydrogen bonding.

Further modification in a different solvent is not possible since the original particle size distribution can't be re-obtained after drying and any solvent change would cause irreversible agglomeration. Moreover toxic solvents and surfactants reduce bio-compatibility [4] and therefore CTAC should be avoided in future preparation for MNPs used in bio-medical applications. However SDS might be selectively removed from the MNP dispersion by precipitation at low temperatures [6], which was observed in one sample. Non-ionic surfactants could also be used, but shouldn’t contain PEO groups since they might precipitate at elevated temperature of 80°C [6]. In difference to the surfactant, co-surfactants like n-butanol could be easily evaporated and won't be a problem in future recipes. Improvement of present preparation method for MNPs using Fenton's reagent has to focus on the polymer in order to decrease the particle size towards 20 nm while increasing their steric stabilization.

6 Acknowledgment

I want to thank Prof. Dr. Niyazi Bicak for giving me the opportunity to come to Istanbul Technical University and to work at his research laboratory on this challenging master thesis project, whereas Martin Andersson provided me with good supervision from Chalmers. Prof. Dr. Hale Gürbüz helped me to carry out the DLS measurements, which were so essential for this project and Prof. Dr. Orhan Kamer helped me in the same way with the VSM measurement. When I came to Chalmers to carry out some analysis, Johan Karlsson was there for me and helped me with TEM as well as Anders Mårtensson, who carried out the TGA with me. Moreover I want to thank Anne Wendel for carrying out the ESCA/XPS analysis. Last but not least I want to thank Bünyamin Karagöz, Ahmet İnce, Hasan Onur Erdem, Barış Kumru, Erdem Sari, Ece Tükenmez, Berkay Demiralp, Gülce Öngör and Yalın Kocaoğlu for helping me with all smaller and bigger problems in laboratory and daily life in Istanbul.

7 References

[1] An-Hui Lu, E. L. Salabas, Ferdi Schüth; Magnetic Nanoparticles: Synthesis, Protection, Functionalization, and Application; Angew. Chem. Int. Ed. 46 (2007) 1222 – 1244

[2] R. Kurchania, S. S. Sawant, R. J. Ball; Synthesis and Characterization of Magnetite/Polyvinyl Alcohol Core-Shell Composite Nanoparticles; J. Am. Ceram. Soc. (2014), 97 [10] 3208–3215

[3] L. Cademartiri, G. A. Ozin, J. Lehn; Concepts of Nanochemistry;
Wiley-VCH Verlag GmbH & Co. KGaA (2009) pp. 173

[4] P. Majewski B. Thierry; Functionalized Magnetite Nanoparticles—Synthesis, Properties, and Bio-Applications; Critical Reviews in Solid State and Materials Sciences, (2007) 32:203–215

[5] P. A. Dresco, V. S. Zaitsev, R J. Gambino, B. Chu; Preparation and Properties of Magnetite and Polymer Magnetite Nanoparticles; Langmuir (1999) Vol. 15, No. 6, 1945-1951

[6] K. Holmberg, B. Jönsson, B. Kronberg, B. Lindman; Surfactants and Polymers in Aqueous Solution; John Wiley & Sons, Ltd. (2002) pp. 1, 139, 178, 181, 197, 204, 261, 277

[7] T. Viegas et al. ; Polyoxazoline: Chemistry, Properties, and Applications in Drug Delivery; Bioconjugate Chem. (2011), 22, 976–986

[8] M. A. Masuelli; Mark-Houwink Parameters for Aqueous-Soluble Polymers and Biopolymers at Various Temperatures; J. of Polymer and Biopolymer Phy. Chem. (2014) Vol. 2, No. 2, 37-43

[9] T. Miyazaki et al.; Role of boric acid for a poly (vinyl alcohol) film as a cross-linking agent: Melting behaviors of the films with boric acid; Polymer 51 (2010) 5539-5549

[10] K. Liu, Z. Wang; A novel method for preparing monodispersed polystyrene nanoparticles; Front. Chem. China (2007) 2(1); 17-20

[11] L. E. Smart, E. A. Moore; Solid state chemistry; CRC Press Taylor & Francis (2005) pp. 412, 427-429

[12] C. O. Metin, L. W. Lake, C. R. Miranda, Q. P. Nguye; Stability of aqueous silica nanoparticle dispersions; J. Nanopart Res (2011) 13:839–850

[13] V. Kuperman; Magnetic Resonance Imaging: Physical Principles and Applications;
Academic Press (2000) pp.1-7; pp. 57-59, 64-66

[14] N. Sim et al.; Responsive MR-imaging probes for N-methyl-Daspartate receptors and direct visualisation of the cellsurface receptors by optical microscopy; Chem. Sci., (2013), 4, 3148

[15] Ilsu Rhee, Chan Kim; Nanoparticle Concentration Dependence of the T1 and T2 Times of Hydrogen Protons in an Aqueous Colloidal Solution of Superparamagnetic Nanoparticles; J. of the Korean Physical Society, Vol. 42, No. 1, (2003), pp. 175-177

[16] M. Akhtari, A. Bragin, R. Moats, A. Frew, M. Mandelkern; Imaging brain neuronal activity using functionalized magnetonanoparticles and MRI; Brain Topogr. (2012) ;25(4)374-88

[17] T. Hosono, H. Takahashi, A. Fujita, R. Joseyphus, K. Tohji, B. Jeyadevan; Synthesis of magnetite nano-particles for AC magnetic heating; J. of Magnetism and Magnetic Mat. 321 (2009) 3019–3023

[18] R. M. Cornell, U. Schwertmann, The Iron Oxides – Structure, Properties, Reactions, Occurrences and Uses; Wiley-VCH Verlag GmbH & Co. KGaA; (2003) 2nd Edition pp. 5, 123, 146, 169

[19] W. Cai, J. Wan; Facile synthesis of superparamagnetic magnetite nanoparticles in liquid polyols; Journal of Colloid and Interface Science 305 (2007) 366–370

[20] I. Robinson et al. ; Synthesis of core-shell gold coated magnetic nanoparticles and their interaction with thiolated DNA; Nanoscale (2010) Dec 2 (12) 2624-30

[21] C. Walling; Fenton's reagent revisited; Acc. Chem. Res. (1975), 8 (4), pp 125–131

[22] E. L. Jenner; α,α,α',α'-Tetramethyltetramethylene glycol; Org. Synth. (1960), 40, 90

[23] K. Barbusinski, Fenton reaction - Controversy concerning the chemistry; Ecological Chemistry and Engineering S. (2009) Vol. 16, No. 3 pp 347-358

[24] A. V. Tolchev et al. ; Temperature and pH effect on composition of a precipitate formed in $FeSO_4$-H_2O-H^+/OH^--H_2O_2 system; Materials Chemistry and Physics 74 (2002) 336–339

[25] N. Bicak et al. ; unpublished results

[26] Malvern Instruments Ltd; Dynamic Light Scattering (DLS) (retrieved 06.12.2014) http://www.malvern.com/en/products/technology/dynamic-light-scattering/default.aspx

[27] J. Crangle, G. M. Goodman; The Magnetization of Pure Iron and Nickel; The Royal Society; (1971) Volume: 321 Issue: 1547

[28] Thermo Scientific; XPS Interpretation; http://xpssimplified.com/periodictable.php (retrieved 27.01.2015)

[29] P. Louette, F. Bodino, J. Pireaux; Poly(vinyl alcohol) (PVA) XPS Reference Core Level and Energy Loss Spectra; Surface Science Spectra vol 12 (2005), 106-110

[30] J. E. Bristol, H. K. Inskip; Preparation of highly alcoholyzed polyvinyl alcohol; US 3541069 A (1968)

8 Appendix

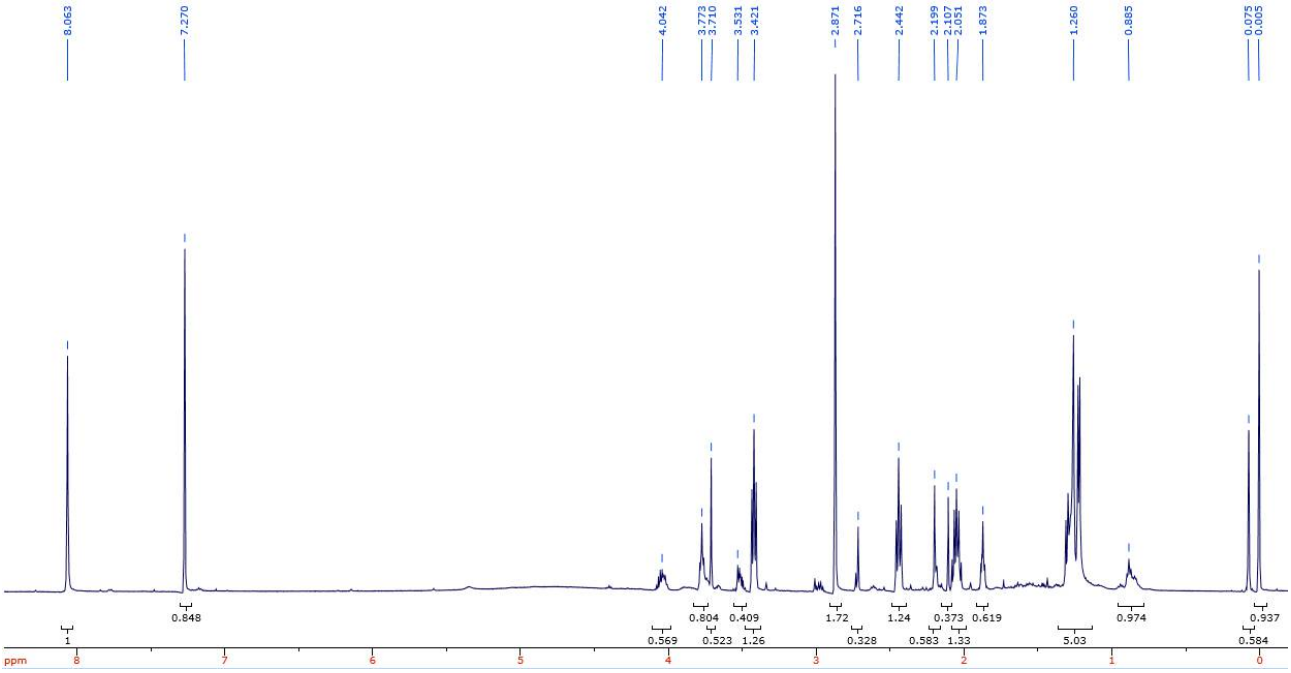

Figure 18 NMR spectra after treating isopropyl alcohol with fentons reagent

8.1 Viscosimetry

$$Solvent: \ water$$

$$T = 30\,°C$$

$$\eta_0 = 0.8007\ cP$$

$$t_0 = 91.3\,s$$

Table 7 Viscosity measurements

c in g · L^{-1}	t in s	η in cP	η_{red} in mL · g^{-1}
2	99.3	0.87	43.8
5	112.7	0.99	46.9
6.25	119.8	1.05	49.9
7.1	124.5	1.09	51.2
8.3	129.1	1.13	49.9
10	139.6	1.22	52.9

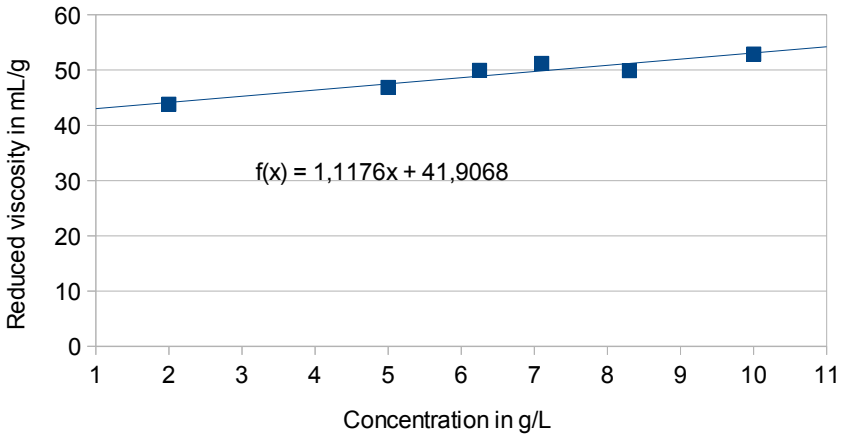

Figure 19 Determination of intrinsic viscosity

$$[\eta] = 41{,}9$$

$$\alpha = 0.65 \qquad [18]$$

$$K = 0.0512 \ cm^3 \cdot g^{-1} \qquad [18]$$

$$\overline{M_V} = 30300 \ g \cdot mol^{-1}$$

8.2 Synthesis of chain transfer agent

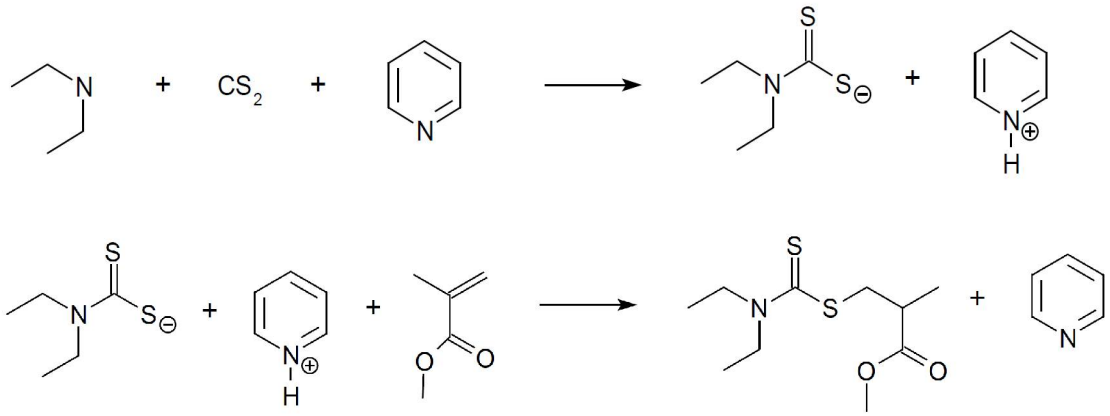

Reagents:

- methanol
- diethylamine 73.14 g/mol
- carbon disulfide 76.14 g/mol

- pyridine 79.1 g/mol
- methyl methacrylate 100 g/mol

Procedure:

7.91 g pyridin (0.1 mol) and 7.31 g diethylamine (0.1 mol) are added to 20 mL of methanol as solvent. Under stirring and cooling by an ice bath 7.61 g carbon disulfide (0.1 mol) are dropwise added and the solution should become slightly yellow or orange. Afterwards 10.0 g methyl methacrylate (0.1 mol) are added and the reaction mixture is heated under reflux at 50°C for 5 hours. For a better yield the reaction is continued at room temperature for 24 h. The product is washed several times with sodium chloride solution, extracted with ether and dried with sodium sulfate (anhydrous). Ether is distilled off and under vacuum at 80°C possible contaminants are removed.

8.3 Polymerization of vinyl acetate

Reagents:

- 1,4 dioxane (re-distilled)
- vinyl acetate 86.09 g/mol
- chain-transfer agent 249.3 g/mol
- AIBN 164.2 g/mol

Procedure:

Polyvinyl acetate is prepared by Reversible addition−fragmentation chain-transfer (RAFT) polymerization of vinyl acetate. The ratio of monomer to chain transfer agent to initiator is 100 : 1 : 0.5 . The reaction is carried out in a 500mL three neck round bottom flask with a reflux condenser at 65°C using re-distilled 1,4 dioxane as solvent. Vinyl acetate is distilled before use and approximately 25 mL are added to 50 mL 1,4 dioxane. The Chain-transfer agent is added and the reactant mixture is flushed with nitrogen to remove any oxygen. For example 25 g vinyl acetate (0.29 mol) require 0.75 g (3 mmol) chain transfer agent and 0.25 g AIBN. After initiator addition the reaction mixture is heated to 65°C and left at this temperature for 9 h. Afterwards the reaction mixture is precipitated in water, washed several times with water and dried in vacuum at 60°C. Determination of molecular weight was carried out by Gel Permeation Chromatography.

Polymer Laboratories
PL GPC Software

22:10 Wed Apr 15 2015

Unknown RUN99.001
2,0 PVAc

Acquired : 21:24 Wed Apr 15 2015
Operator POLYMERLAB

Concentration :
Injection Volume :
Solvent : THF
Column Set : WATERS HR 5E, 4E, 3, 2 narowbore

Detector : Agilent 1100 RI detector
Temperature : 30 C
Flow Rate : 0.300
Standards : Polystyrene standards

Method 8
Comments : Injection Vol : 20 microlitre (BHT Marker)

Calibration Using : Narrow Standards
Calibration Limits : 30.15 to 49.35 Mins
Flow Rate Marker : found at : 49.36

Curve Used : 4th Order Polynomial
Last Calibrated : Mon Mar 02 16:26:06 2015
in Standards at : 49.62 Mins

Broad Peak Start : 31.28 End : 45.60 Mins

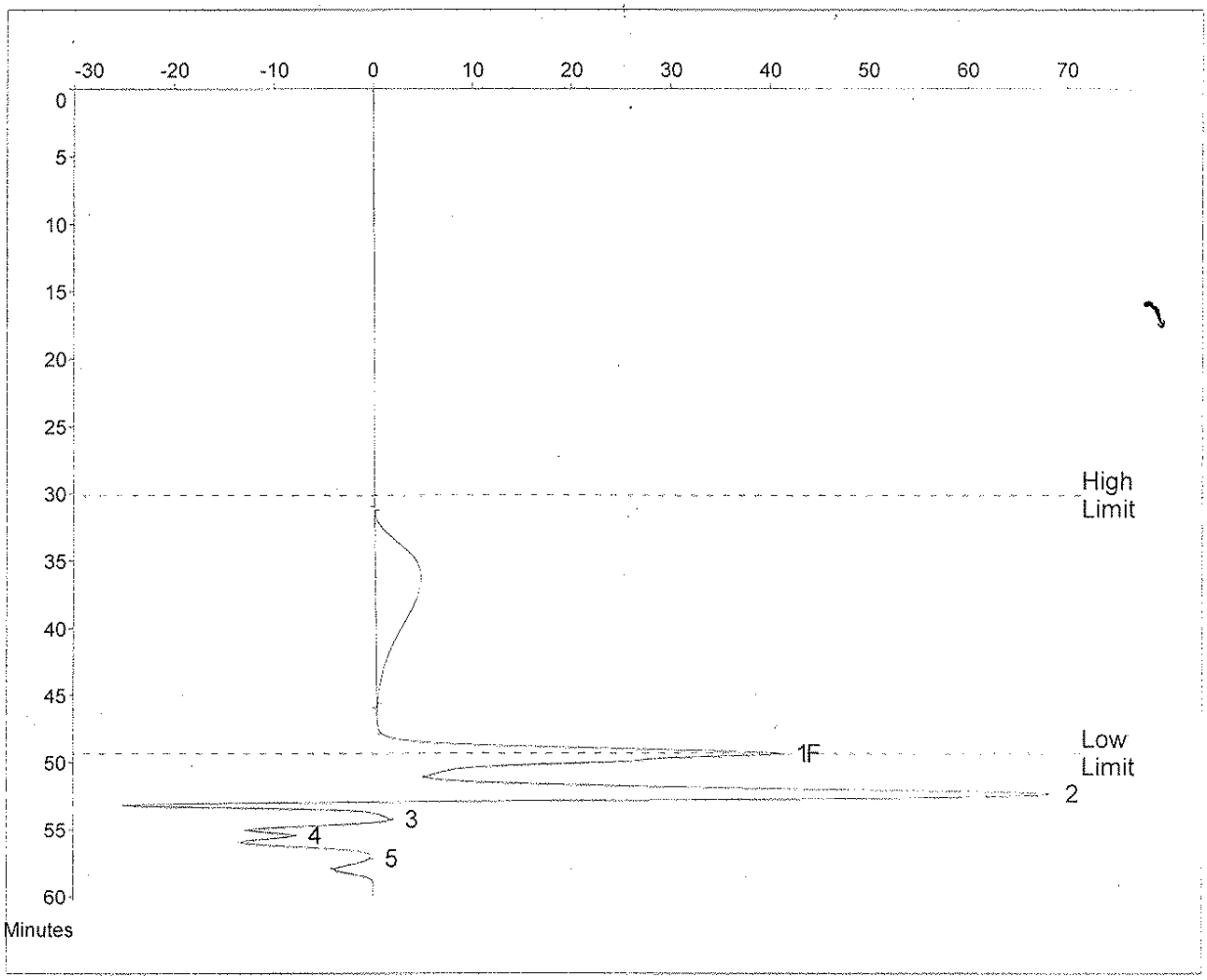

Molecular Weight Averages

Mp =	15142	Mz =	27251
Mn =	8197	Mz+1 =	41885
Mw =	15992	Mv =	14655
Polydispersity =	1.951	Peak Area =	1596464

8.4 Preparation of PVAL by methanolysis of polyvinyl acetate

Reagents:

- polyvinyl acetate
- methanol
- metallic sodium

Procedure:

Polyvinyl acetate is dissolved in methanol, whereas 20 g require 100 mL of methanol. A sodium methoxide solution is prepared by stepwise addition of 0.1 g sodium to 10 mL of methanol. Addition of sodium methoxide solution to the polymer solution should start the reaction followed by a color change and slight temperature increase. The reaction is carried out for 2 h under stirring. Afterwards the reaction mixture becomes turbid and might form a gel, which dissolves by addition of small amounts of water. To neutralize remaining sodium methoxide approximately 0.5 ml HCl are added. To facilitate precipitation of polymer the reaction mixture is concentrated by rotary evaporator at 60°C and vacuum. Thereafter Acetone is added and the polymer precipitates, which is then filtered and dried under vacuum at 50°C. The PVAL is expected to be 99-99.5% hydrolyzed and referred as fully hydrolyzed [30].